2854 5-P

THE UNIVERSITY OF MICHIGAN RESEARCH INSTITUTE
ANN ARBOR, MICHIGAN

RESEARCH ON CROSSED-FIELD ELECTRON DEVICES

QUARTERLY PROGRESS REPORT NO. 4

Period Covering September 1, 1959 to December 1, 1959

ELECTRON PHYSICS LABORATORY

Department of Electrical Engineering

291 700

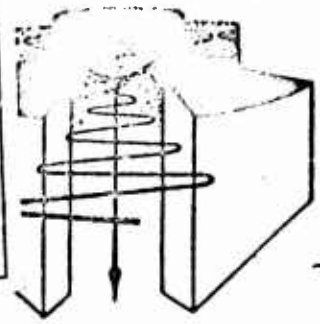

By: R. W. Larson
R. J. Martin
N. A. Masnari
M. H. Miller
J. E. Rowe

Approved By: J. E. Rowe

CONTRACT NO. DA-36-039 sc-78260, SIGNAL CORPS, DEPARTMENT OF THE ARMY, DEPARTMENT OF THE ARMY PROJECT NO. 3-99-15-104, PLACED BY THE U.S. ARMY SIGNAL RESEARCH AND DEVELOPMENT LABORATORY, FORT MONMOUTH, NEW JERSEY.
December, 1959

THE UNIVERSITY OF MICHIGAN RESEARCH INSTITUTE
ANN ARBOR, MICHIGAN

QUARTERLY PROGRESS REPORT NO. 4

FOR

RESEARCH ON CROSSED-FIELD ELECTRON DEVICES

This report covers the period September 1, 1959 to December 1, 1959

Electron Physics Laboratory
Department of Electrical Engineering

By: R. W. Larson
R. J. Martin
N. A. Masnari
M. H. Miller
J. E. Rowe

Approved by: J. E. Rowe
J. E. Rowe, Head
Electron Physics Laboratory

Project 2854

CONTRACT NO. DA-36-039 sc-78260
SIGNAL CORPS, DEPARTMENT OF THE ARMY
DEPARTMENT OF THE ARMY PROJECT NO. 3-99-15-104
PLACED BY THE U. S. ARMY SIGNAL RESEARCH AND DEVELOPMENT LABORATORY
FORT MONMOUTH, NEW JERSEY

December, 1959

ABSTRACT

A discussion of the initial experimental tests on the crossed-field stream analyzer with the potential trap in the sole is presented and some analog computer calculations of electron trajectories through the trap are given. A general verification of previous results has been obtained.

Extensive calculations of beating-wave amplification in the presence of beam space-charge and circuit loss are given and the significance of the results is discussed.

Starting conditions for the M-type BWO are obtained when d = 0 and some interesting aspects with regard to their dependence on H and r are commented on.

A generalized analysis of the two-beam crossed-field amplifier is developed in which the slip between the two beams is accounted for. A physical interpretation of the growth mechanism in such a device is offered.

TABLE OF CONTENTS

LIST OF ILLUSTRATIONS

LIST OF ILLUSTRATIONS (cont'd)

PERSONNEL

Scientific and Engineering Personnel		Time Worked in Man Months*
G. Hok	Professors of Electrical Engineering	.02
M. Miller		1.02
J. Rowe		.40
L. Paul	Research Associate	.16
R. Larson	Graduate Research Assistants	2.84
R. Martin		.84
N. Masnari	Research Assistant	.51
J. Fox	Electronics Technicians	.50
K. McCrath		.33
C. Watkins		.45
Service Personnel		
V. Burris	Administrative Assistant	.65
T. Knopf	Assistant Machine Shop Foreman	.51
R. Casterline	Machinists	.44
M. Tobias		.49
R. Kepler	Laboratory Technicians	.44
J. Spratt		.31
G. Beauchamp	Technical Illustrator	.26
P. Foerster	Secretaries	.79
J. Johnston		.58
J. Marsh		.54

* Time worked is based on 172 hours per month.

QUARTERLY PROGRESS REPORT NO. 4

FOR

RESEARCH ON CROSSED-FIELD ELECTRON DEVICES

1. Purpose

The purpose of this research is to investigate both theoretically and experimentally the operation of crossed-field devices. Particular areas of investigation will be electron interaction with crossed fields in both amplifiers and oscillators, crossed-field injection systems, re-entrant beam devices and r-f structures for high-power crossed-field amplifiers and oscillators. The work on this contract is a continuation of work carried out under DA-36-039 sc-56714.

2. Objectives for the Period (J. E. Rowe)

2.1 Crossed-Field Stream Analyzer. During this period it was planned to modify the cathode design in the crossed-field stream tester, to reassemble the tester and to begin taking experimental data.

2.2 Electron Trajectory Determination. It was planned during this period to complete the construction of additional current source circuitry so that 1584 sources would be available to use in the analysis of a large-scale crossed-field diode. Also new models of Poisson Cells were to be made to use in the analysis of the crossed-field diode.

2.3 Beating-Wave Amplification. As a result of previous investigations it was planned to carry out calculations of both growing-wave amplification and beating-wave amplification in the magnetron amplifier for large values of space charge and finite values of the circuit loss parameter.

2.4 Multiple-Stream M-Type Devices. Previously an analysis of the double-stream crossed-field amplifier was given and a limited number of solutions were presented. It was planned to investigate the operation of this device for various values of ω/ω_c and S in order to gain a clearer understanding of its operation.

2.5 M-Type Backward-Wave Oscillators. During this period it was planned to further investigate M-type backward-wave oscillator starting conditions using a simple one-level treatment of the input boundary value problem.

3. Crossed-Field Stream Analyzer (M. H. Miller, R. W. Larson)

The principal effort this past quarter has been devoted to the experimental analyzer. The troubles with our vacuum system mentioned in the previous quarterly progress report unfortunately continued throughout September. Also the same problems with the cathode strips continued to occur until the middle of October when the strip was firmly wired into place and a more uniform strip became available. During this period the general nature of Miller's results[1] was confirmed, with one exception. Under certain conditions current was present on the sole segments following the potential depression for higher values of the Φ_{oa}/B_o^2 parameter than he had observed. This was probably due to a combination of defocusing, energy exchange in the sole-depression region and an energy exchange along the structure perhaps due to the nonlaminarity of the beam. This last result is also seen in the results of the first stream analyzer.

---

1. Miller, M. H., "Study of High-Temperature Electrons Originating in Streams Flowing in Crossed D-C Electric and Magnetic Fields", Technical Report No. 26, Electron Tube Laboratory, Department of Electrical Engineering, The University of Michigan; July, 1958.

The last half of this period has seen the use of only two cathode strips, although the second of these has recently failed. Rather than give the cathode characteristics for both strips, hereafter labeled "A" and "B", let it suffice to state that both gave very similar results in terms of perveance and volt-ampere characteristics to those of the first stream analyzer[2]. The data on cathode A collected while attempting to obtain large sole currents and note overall behavior was largely exploratory. Figures 3.1 and 3.2 show data for cathode A which unfortunately is incomplete since the general growth in electron temperature with distance is not apparent. Later figures will show this more clearly. Still, it is apparent that there has been a doubling of the temperature in a distance of nine probes, a little over an inch.

At this point it was felt that a good deal of helpful information might be gleaned from a study of analog computer space-charge-free trajectory plots. The first part of November was spent in making trajectory plots using the technique of Rowe[3] and Martin, a few of which are shown in Figs. 3.3 through 3.5. From these curves it is apparent what must be done to have a majority of electrons in the stream travel far into the potential depression. First, the electrons should have a short cycloidal length (low Φ_{ca}/B_o^2), second, they should travel close to the sole and finally, the beam must enter at an optimum point if it is cycloiding although it is preferable that it does not cycloid.

---

2. ibid., Figs. 5.3 and 5.4.

3. Rowe, J. E., and Martin, R. J., "An Electron Trajectory Calculator and Its Component Poisson Cell", Technical Report No. 28, Electron Physics Laboratory, Department of Electrical Engineering, The University of Michigan; September, 1958.

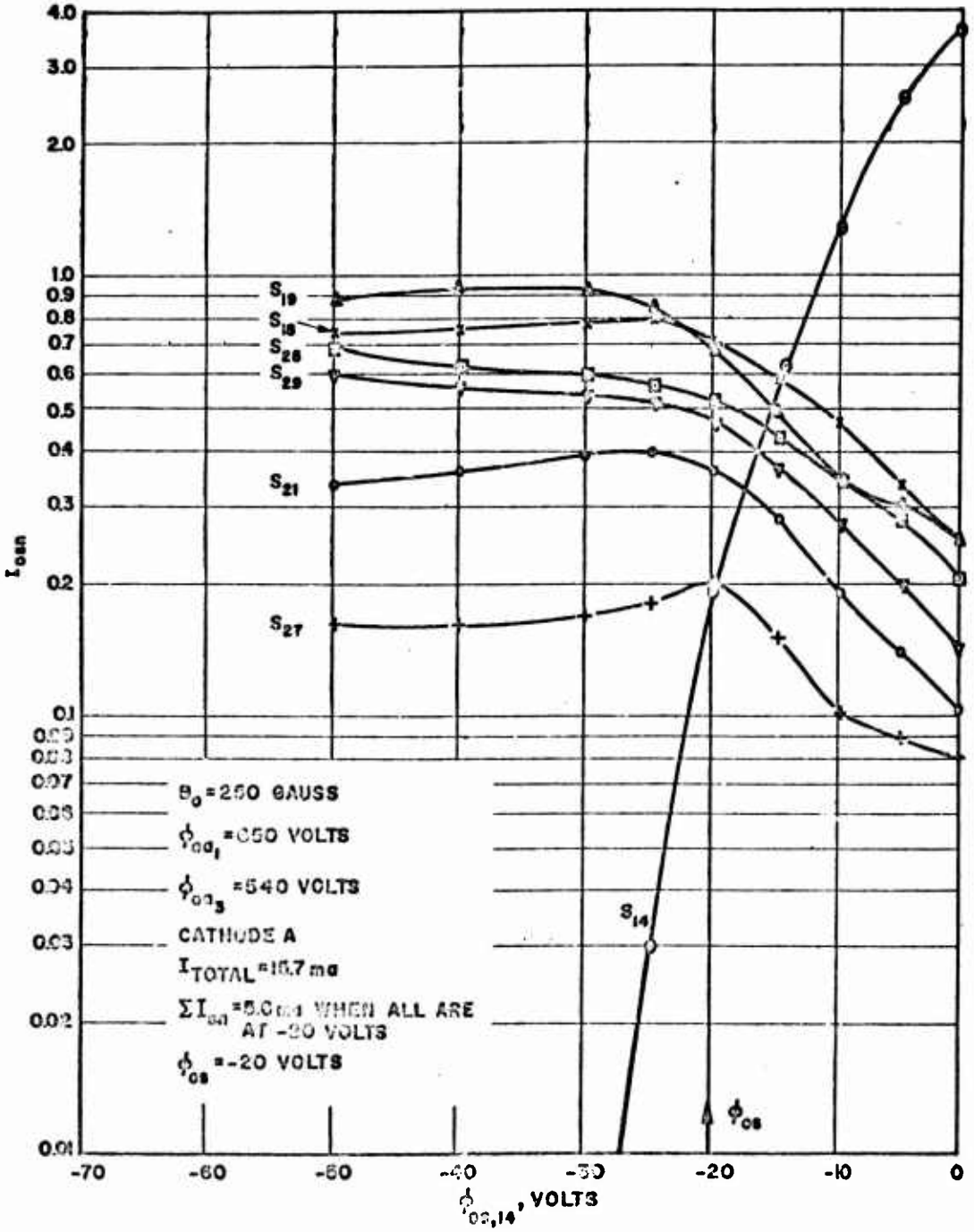

FIG. 3.1 ENERGY DISTRIBUTION CURVES, SOLE SEGMENT NO.14, CATHODE A

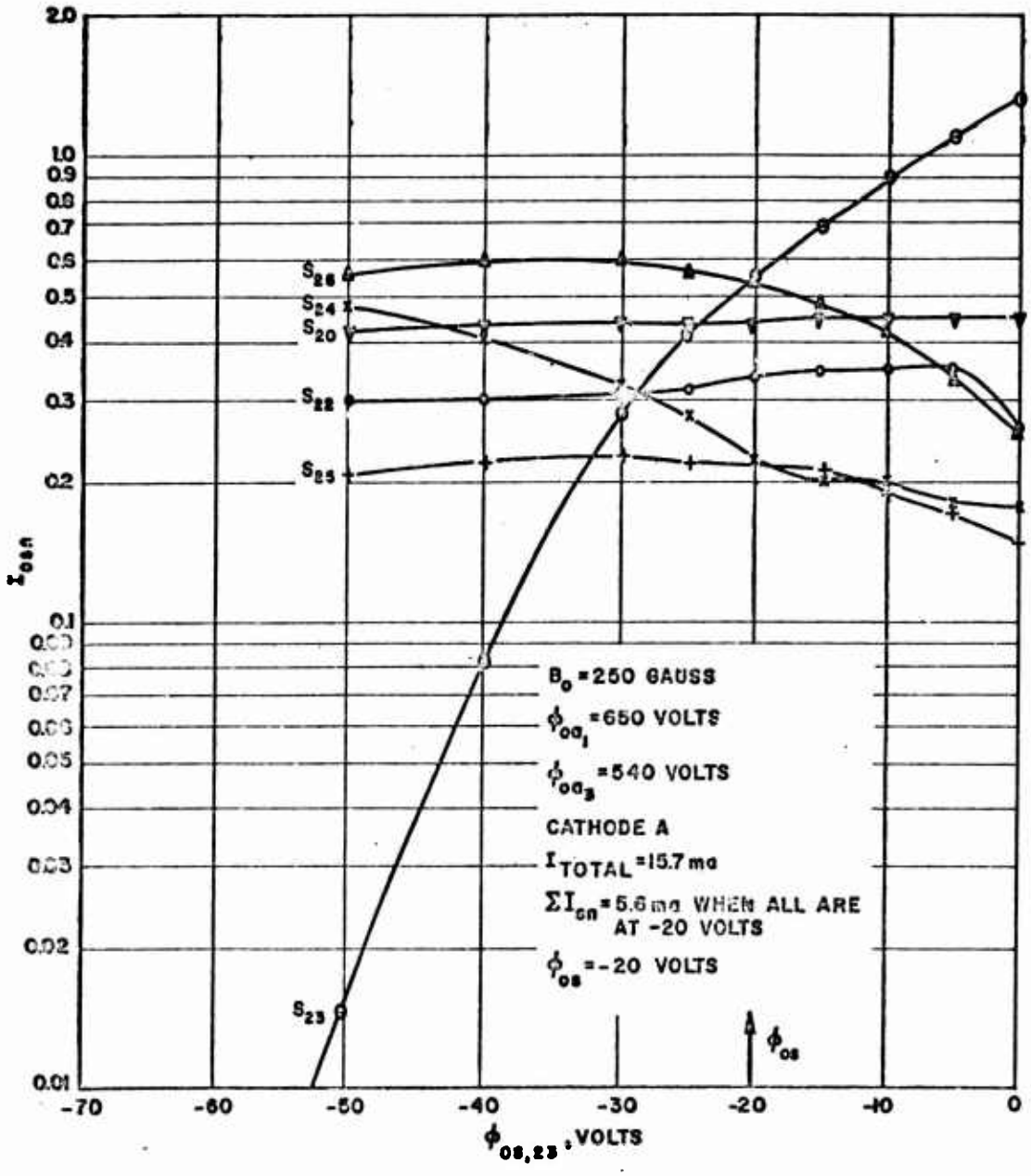

FIG. 3.2 ENERGY DISTRIBUTION CURVES, SOLE SEGMENT NO. 23, CATHODE A

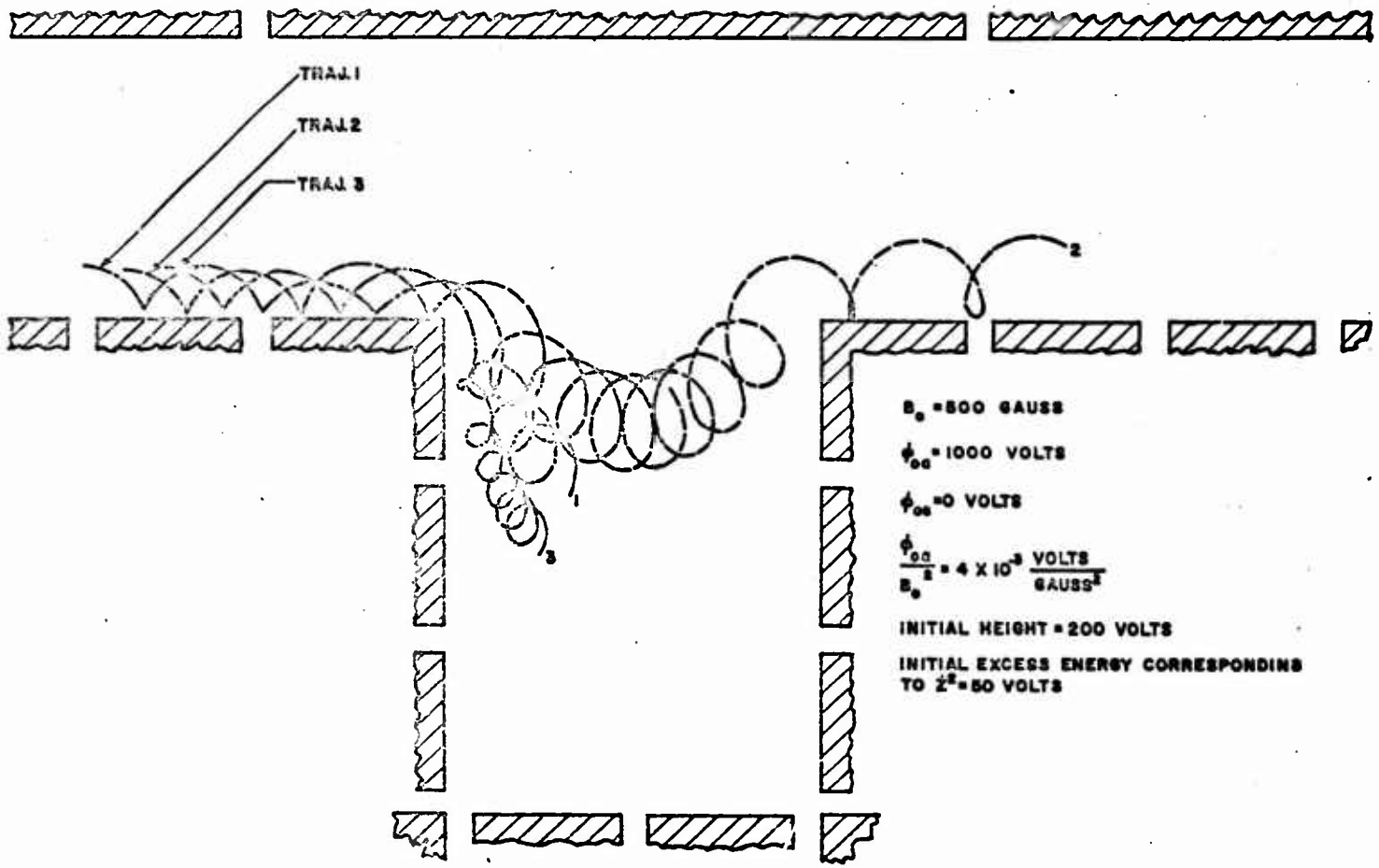

FIG. 3.3 SPACE-CHARGE-FREE ELECTRON TRAJECTORIES IN STREAM-ANALYZER GEOMETRY
(INITIAL POSITION AS PARAMETER)

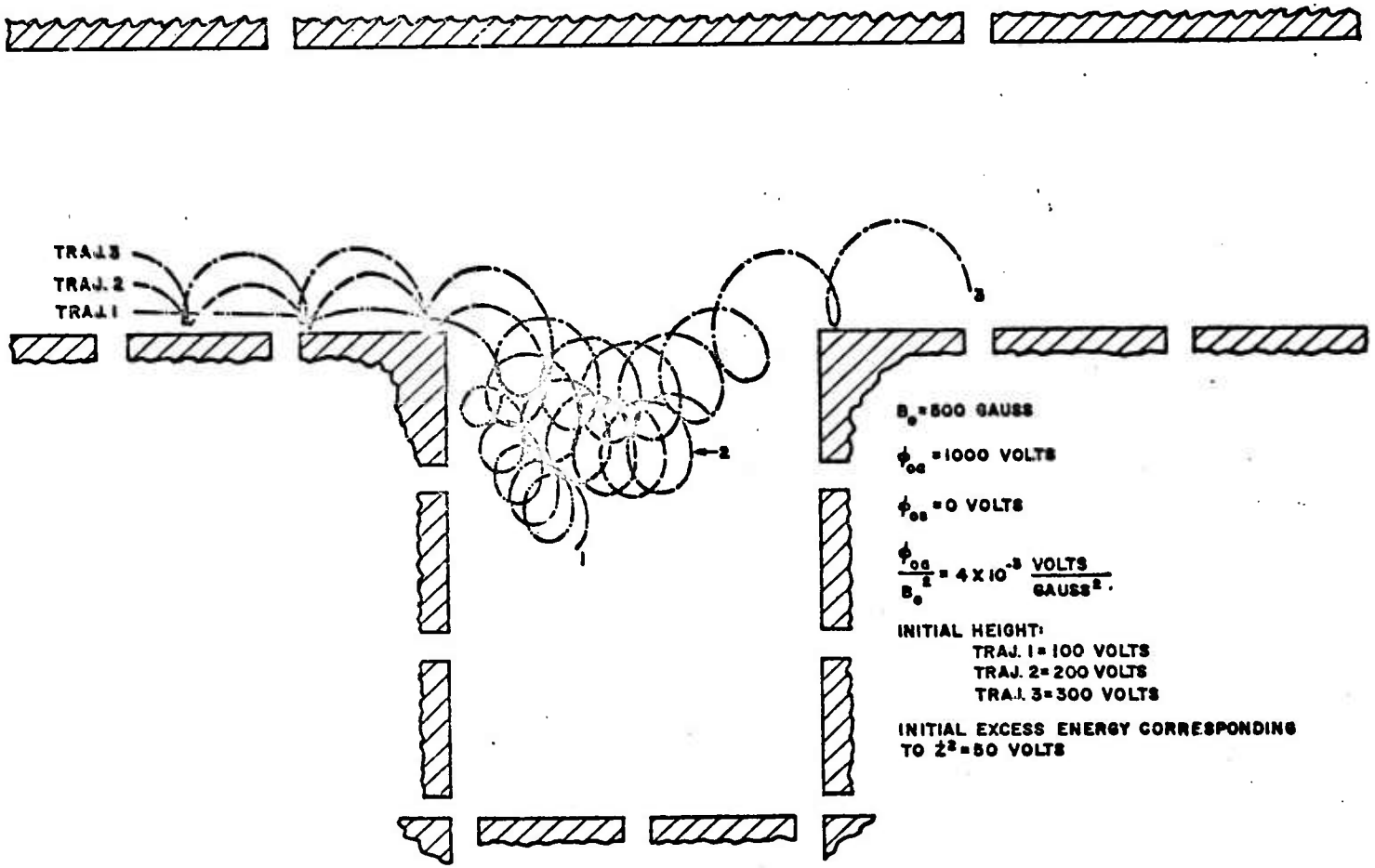

FIG. 3.4 SPACE-CHARGE-FREE ELECTRON TRAJECTORIES IN STREAM-ANALYZER GEOMETRY
(INITIAL VELOCITY AS PARAMETER)

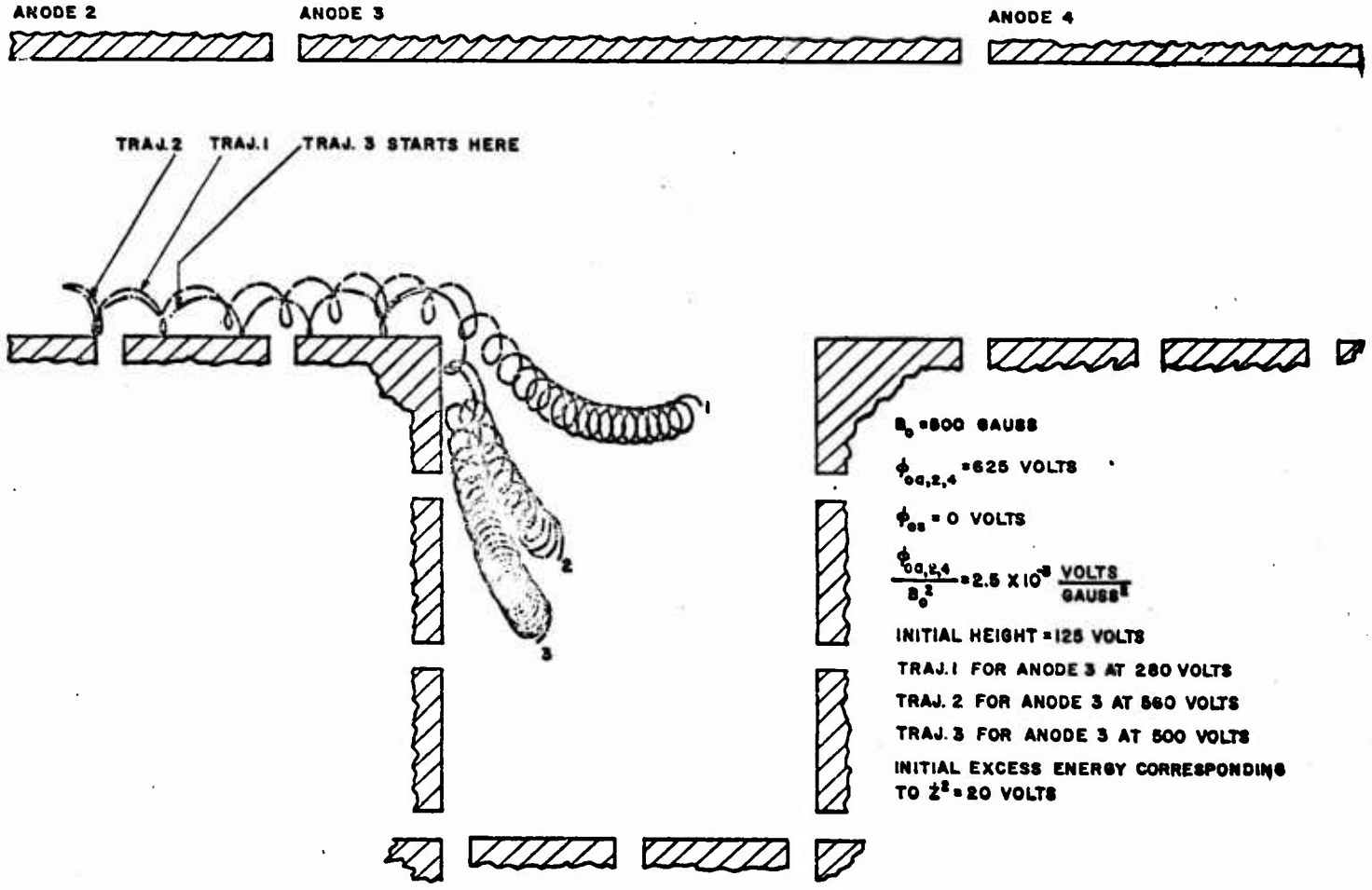

FIG. 3.5 SPACE-CHARGE-FREE ELECTRON TRAJECTORIES IN STREAM-ANALYZER GEOMETRY
(THIRD ANODE VOLTAGE AS PARAMETER)

The last part of November was spent largely in continued exploration into the electron energy as a function of distance for various parameters. Not enough data has been taken to make any conclusions about the cause of the rise in electron temperature with distance, or the variation in temperature across the potential depression.

It has become apparent that in order to study adequately the effect of the potential depression, we must have a more laminar beam. To that end another graphite plate was employed with the analog computer to determine if the existing geometry could be used to get a more nearly laminar beam. Figures 3.6 and 3.7 show the effect of placing the cathode block at a negative potential and the second anode at a lower voltage than the first. Unfortunately we as yet do not have any experimental evidence to correlate with this.

It is obvious that even this electrode potential change is not sufficient to obtain a laminar beam, therefore, further work will be done to find a better cathode configuration. In addition, work will continue on finding a correlation between the energy increase and the various parameter changes. It is hoped that we may soon begin noise studies to correlate with the negative sole current. Additional effort will be devoted also to securing a more reliable filament. An investigation of the use of thoria on tungsten is presently being carried out in an effort to reduce the operating temperature of the cathode.

4. Electron Trajectories in Crossed-Field Devices (J. E. Rowe, R. J. Martin, N. A. Masnari)

Some difficulty developed in the construction of the latest Poisson Cell. This cell is a representation of a large planar crossed-

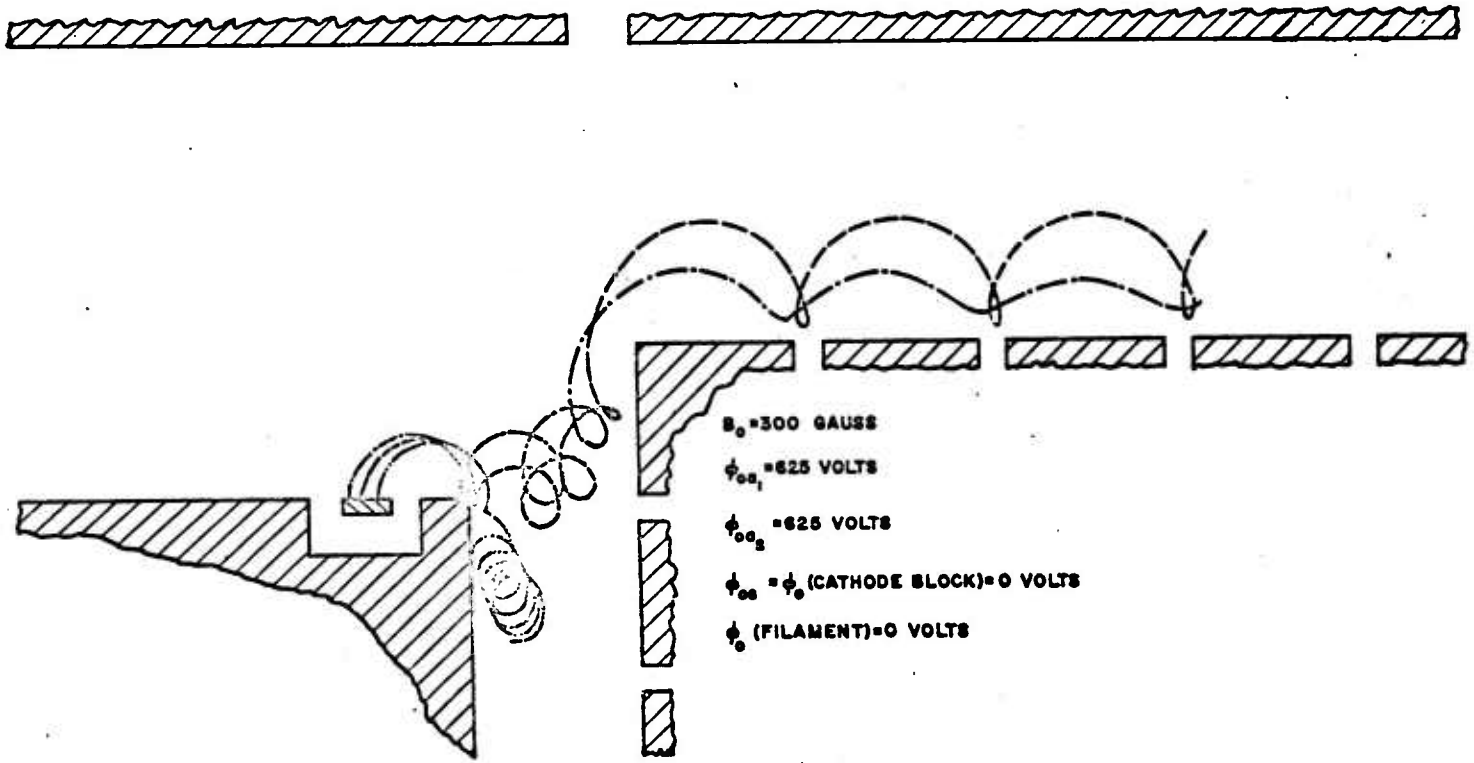

FIG. 3.6 SPACE-CHARGE-FREE ELECTRON TRAJECTORIES IN STREAM-ANALYZER GEOMETRY
(CATHODE REGION TRAJECTORIES)

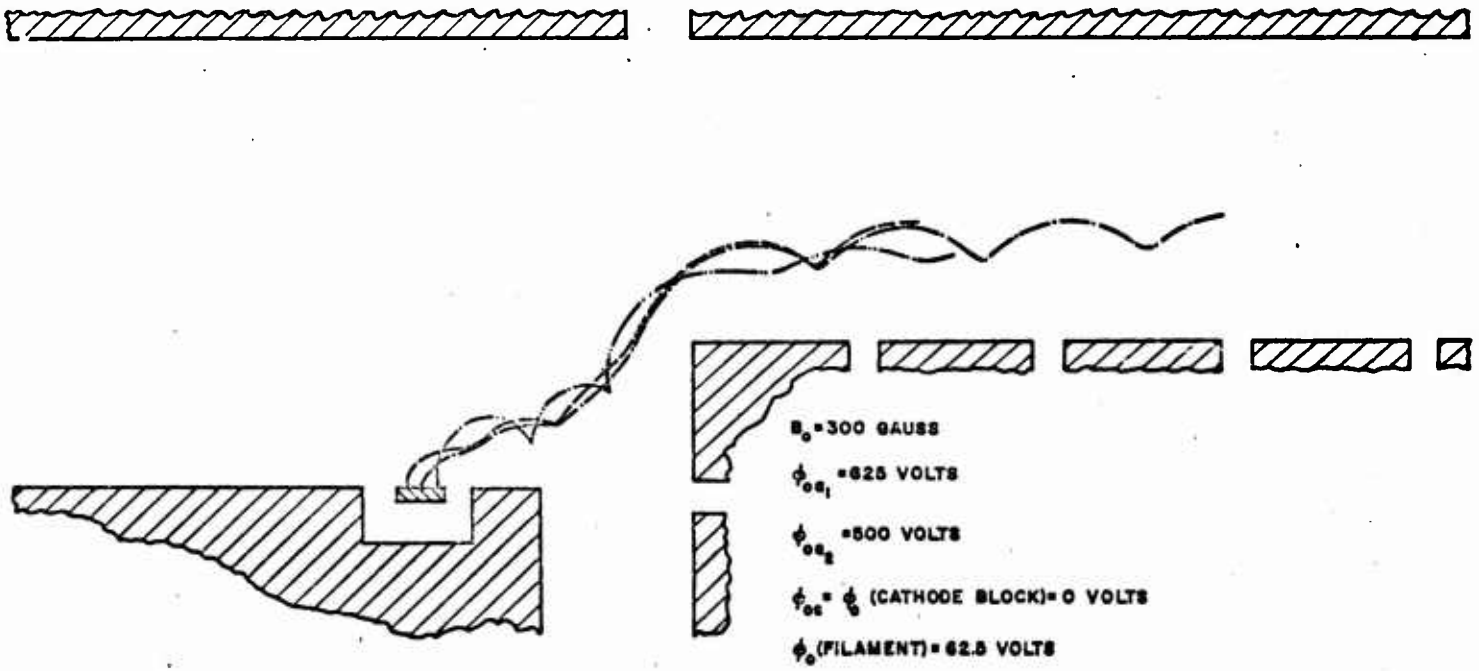

FIG. 3.7 SPACE-CHARGE-FREE ELECTRON TRAJECTORIES IN STREAM-ANALYZER GEOMETRY
(CATHODE REGION TRAJECTORIES)

field diode with provision for injecting space charge throughout the entire region of the diode. In making connection from the space-charge simulating current sources into the cell, difficulty was encountered that would be traced to two causes. First, the method used in making the connection between current sources and cell will be discussed, then the encountered difficulties will be covered, and the steps taken to alleviate the difficulties will be presented.

To make the current source to Poisson Cell connections a lamicoid pattern of the Poisson Cell current-sources configuration is first prepared. This pattern is utilized to determine the spacing and size of each source when the sources are silver printed upon the graphite-Hydrostone place. The lamicoid pattern is then glued to the plate. Leads from the current-sources control panel are soldered through the lamicoid pattern to the silver print dots using Wood's metal and soldering flux. In this manner the pattern serves as a means of mechanically holding the current-sources leads so that the leads will not be pulled from the Poisson Cell. The process of making these current-source connections is quite time-consuming. However, a better method to effect a large saving in time has yet to be devised. The primary difficulty has been the fact that each cell has a different current sources configuration.

There were two difficulties associated with the construction of the latest Poisson Cell. One was that sources would tend to short to each other in making the solder-to-silver-dot connection. The other difficulty was that at some later time these connections would open up. These problems occur because the underside of the graphite-Hydrostone plate is not perfectly flat, and because flexing can occur

between the plate and the lamicoid pattern. In the first case, while soldering, solder tends to flow between the pattern and the plate causing shorting of solder connections. In the second case, forces occur that are great enough to break the silver-dot-to-solder connections, causing open circuits.

To alleviate the above difficulties a variation in applying the lamicoid pattern to the Poisson Cell will be used. One surface of the pattern will be heavily loaded with liquid adhesive and then applied to the under surface of the Cell. In this manner the Cell and pattern will be one integral unit with no open space between them. This will prevent shorting of soldered connections and minimize the possibility of connections opening. Additional time will be required to clean adhesive out of the holes in the pattern before making current source connections. However, the increased reliability of the procedure will actually decrease the time required to produce a Poisson Cell.

During the last period a considerable amount of time was spent using the computer and Poisson Cell equipment to aid in the design of various electron gun systems for crossed-field tubes and also in the study of electron motion in the crossed-field stream analyzer reported in section 3 of this report. This work to some extent held up the work on the large crossed-field diode.

The major concern at the present time is the completion of the planar-diode Poisson Cell and the analysis of its space-charge limited operation. Following investigation of the diode, a crossed-field Poisson Cell will be constructed and analyzed. This tube, similar to those previously investigated, will have two improvements: a larger magnification (larger geometry) and a variable cathode position. The larger geometry

will allow a finer control of the space-charge representation and the movable cathode will permit the determination of the optimum cathode position for a given beam and space-charge density distribution.

Poisson Cells will be continually produced and investigated for linearity and resistivity in the desired range.

5. Beating-Wave Amplification in M-Type Devices (J. E. Rowe)

Previously the gain equations for the magnetron amplifier were developed and various solutions of the secular equation and the gain equation were presented to illustrate both growing-wave and beating-wave amplification in M-type devices. All previous calculations were for zero circuit loss. A significant beating-wave gain was shown in the past report for various values of the beam position parameter and the space-charge parameter. The effect of circuit loss on the beating-wave gain will be shown in this section.

It is convenient to transform the previous secular equation using the definition $\delta = j\ell$ into one of the more familiar form where $\delta = x + jy$.

$$\delta^3 - j\left[2r\frac{(H-1)}{(H+1)} + (b-jd)\right]\delta^2 - \left[r^2 + 2r(b-jd)\frac{(H-1)}{(H+1)} + 1\right]\delta$$

$$+ j(b-jd)r^2 = 0 \quad . \qquad (5.1)$$

where

$$H = \frac{\tanh j\Gamma(y_d - y_b)}{\tanh j\Gamma(y_a - y_s)} \quad ,$$

$$r = \frac{s_u}{D} \quad ,$$

and

d = the circuit loss parameter.

The wave amplitudes are computed as outlined in the previous report and the gain as a function of length is given by

$$\frac{V_t(\theta)}{V_a} = e^{-j\frac{\theta}{D}} \sum_{n=1}^{3} \frac{V_n}{V_a} e^{-\theta\delta_n} \qquad (5.2)$$

where $\theta = 2\pi DN$.

Solutions of the secular equation for particular values of H, r and d are shown in Figs. 5.1 and 5.2. It is seen that the real parts of the propagation constants for the growing and declining waves do not go exactly to zero as they do in the zero loss case. Their value for large values of b does become extremely small and for all practical purposes can be considered zero. Even in the finite circuit loss case there are regions in which beating-wave amplification can and does occur. The gain as computed through Eq. 5.2 is shown in Figs. 5.3 through 5.6 for representative values of H, r and d.

As in the case of no circuit loss it is seen that beating-wave amplification occurs for b greater than 2.0 and decreases with increasing b. When there is loss on the circuit, succeeding maxima are smaller than the first, and hence it is desirable to operate at the first maximum to obtain maximum gain and the shortest device length. As the space charge is increased the b for beating-wave gain becomes higher and the gain decreases. At very high values of space charge and large b the gain exhibits oscillatory tendencies near the input to the amplifier and then exhibits growing-wave gain as illustrated in Fig. 5.6. This gain is largely drift-space gain.

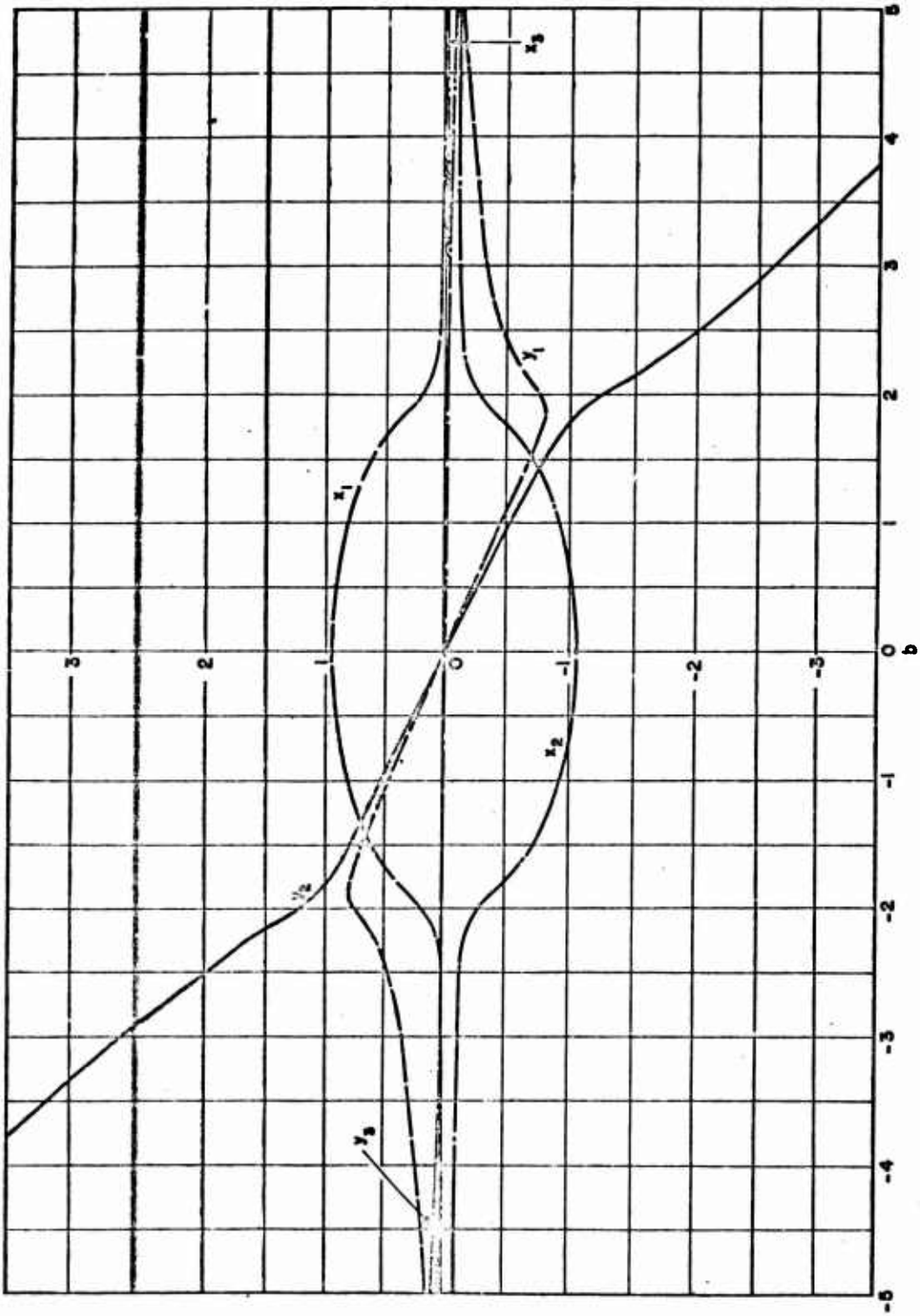

FIG. 5.1 M-TYPE AMPLIFIER PROPAGATION CONSTANTS. (H=1, r=0.1, d=0.1)

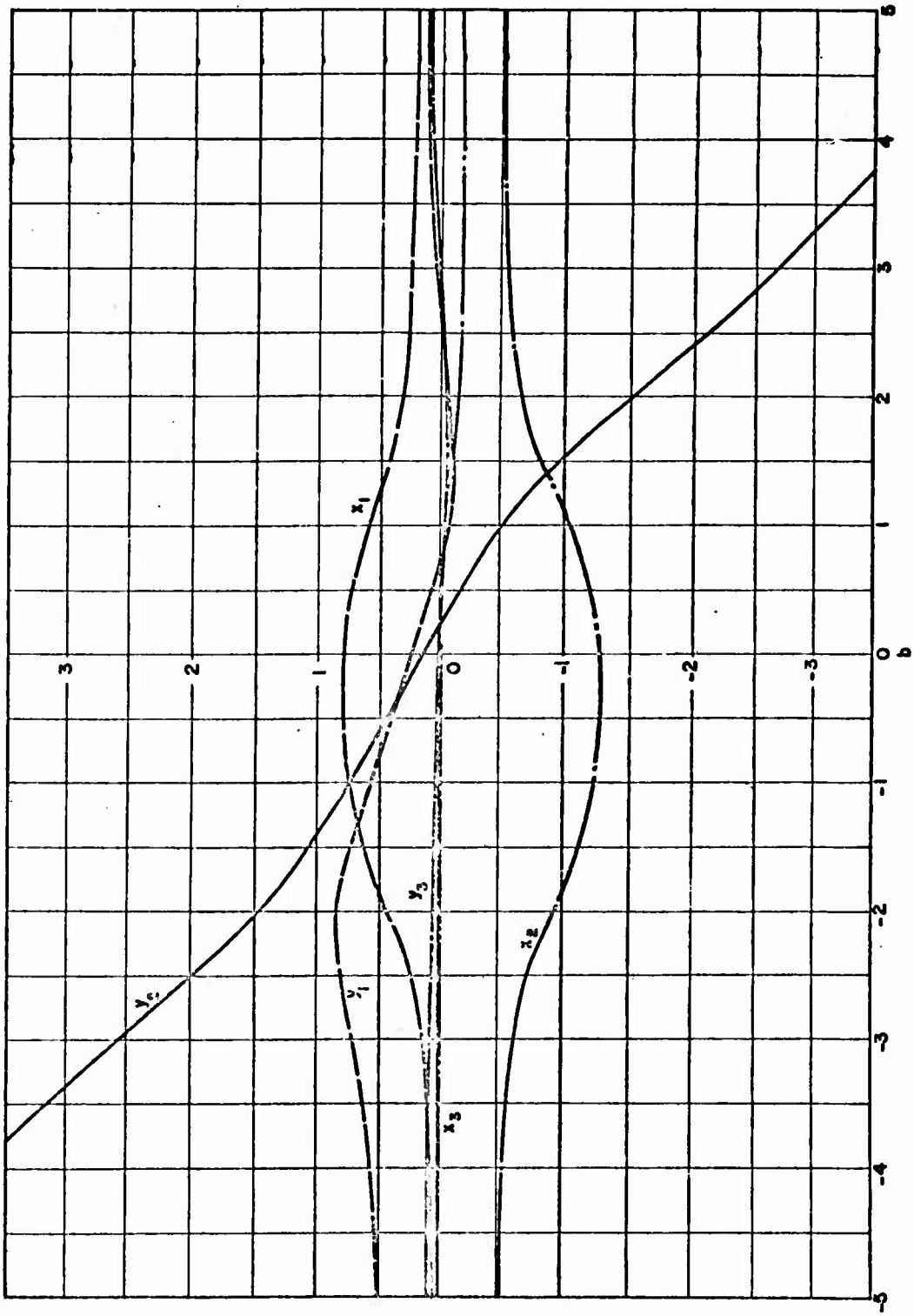

FIG. 5.2 M-TYPE AMPLIFIER PROPAGATION CONSTANTS. (H=0.05, r=0.2, d=0.5)

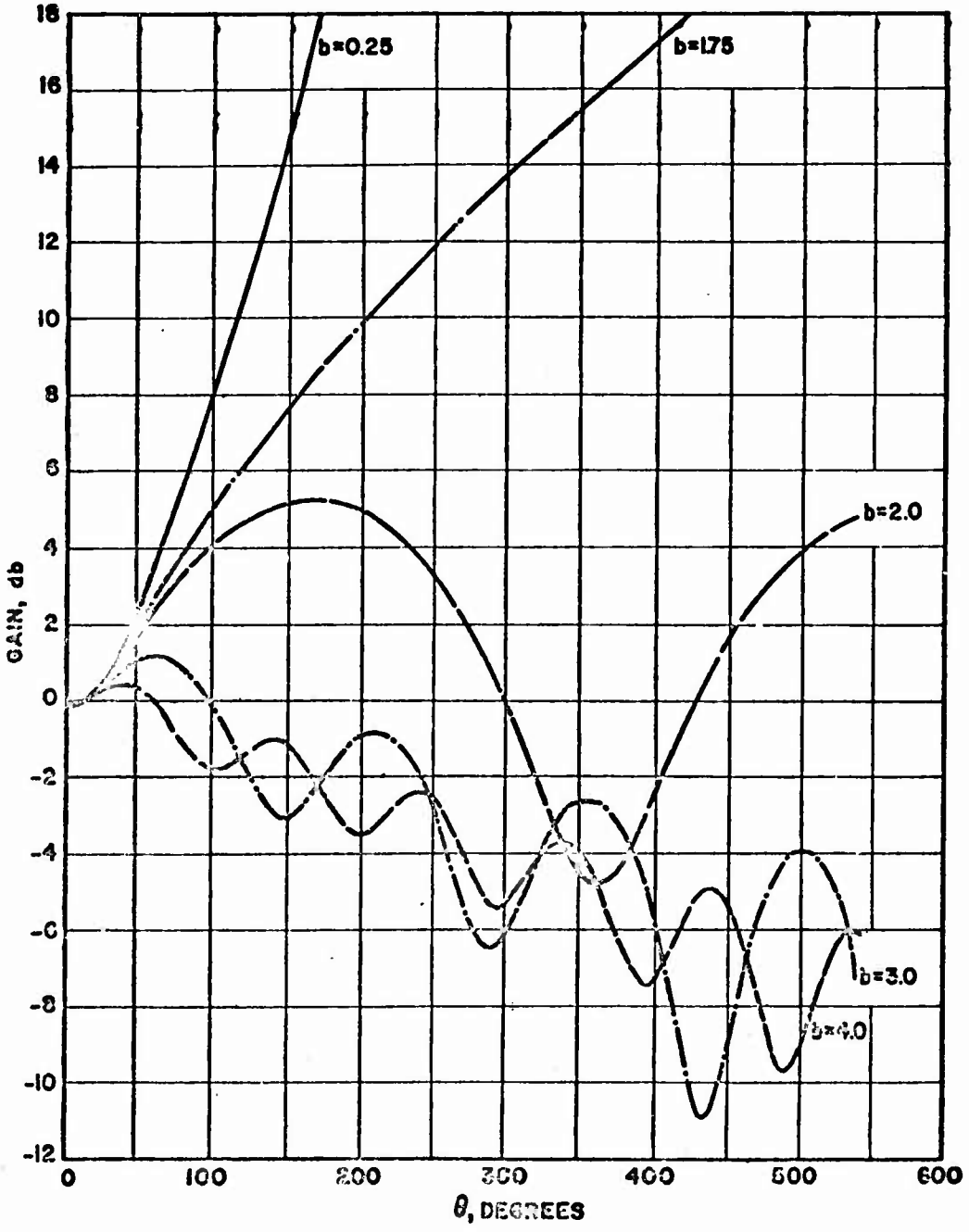

FIG. 5.3 GAIN VS. θ FOR THE M-TYPE AMPLIFIER.
(H=0.05, r=0.1, d=0.1)

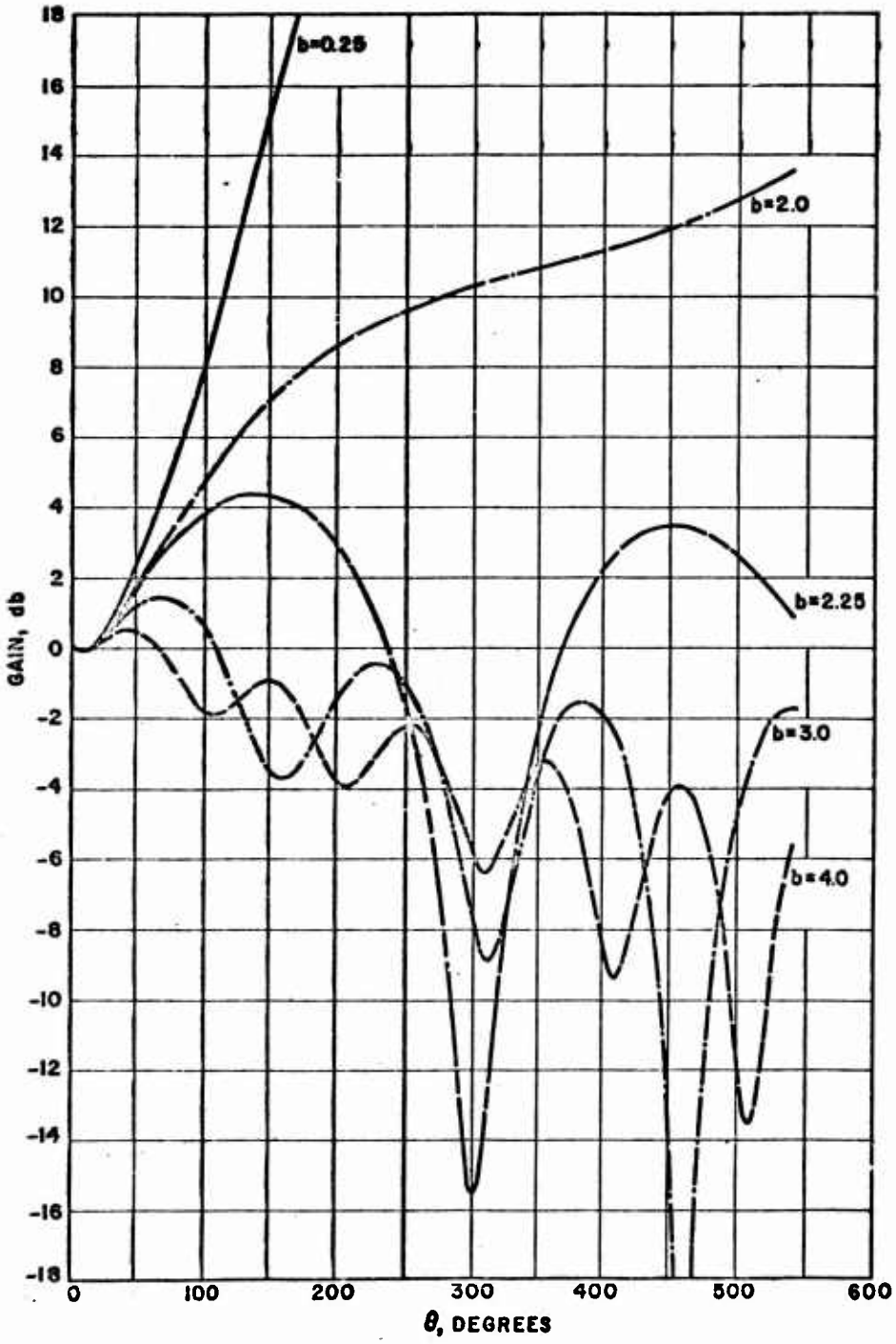

FIG. 5.4 GAIN VS. θ FOR THE M-TYPE AMPLIFIER. (H=1, r=0.2, d=0.1)

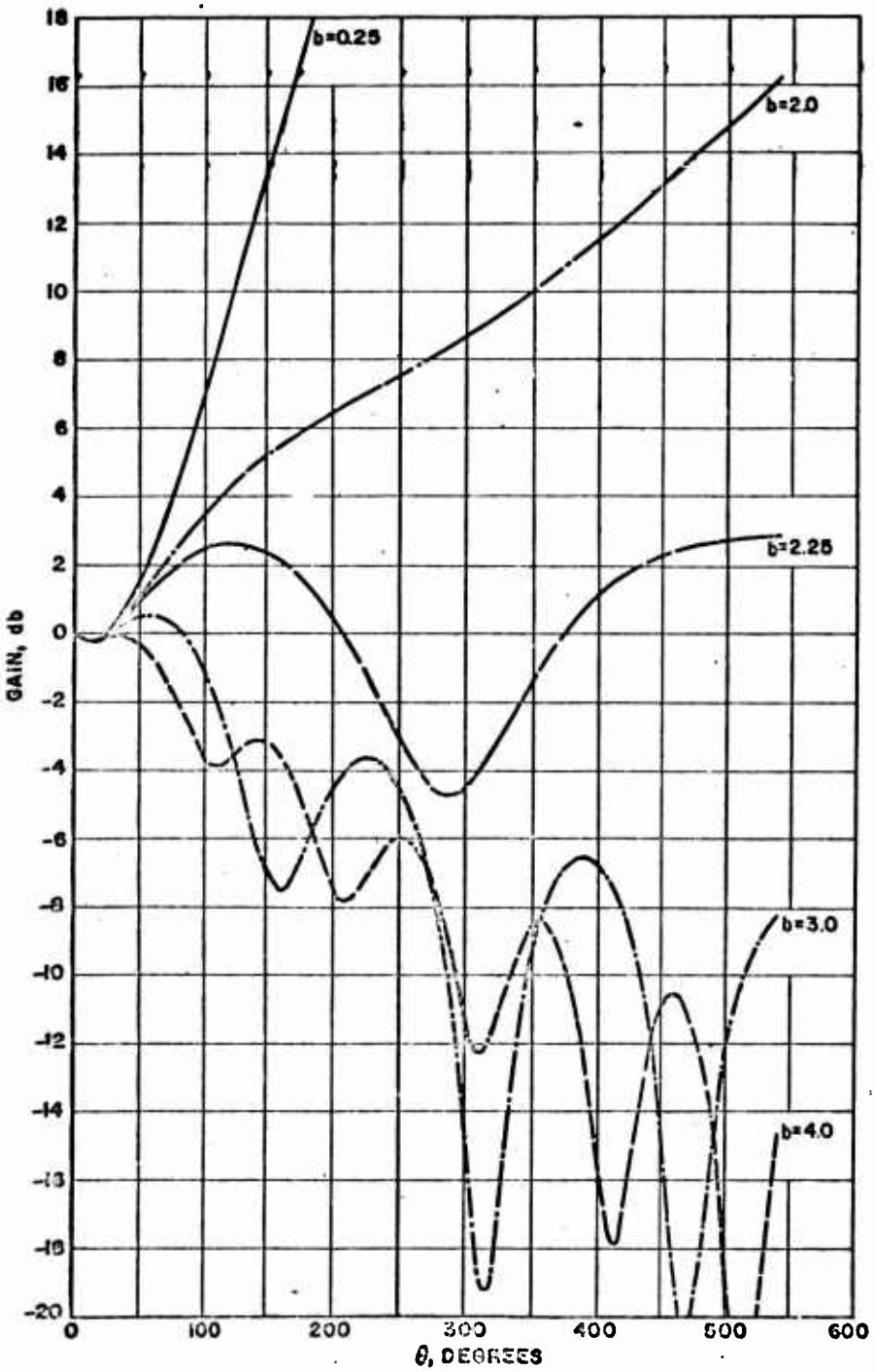

FIG. 5.5 GAIN VS. θ FOR THE M-TYPE AMPLIFIER.
(H=1, r=0.1, d=0.2)

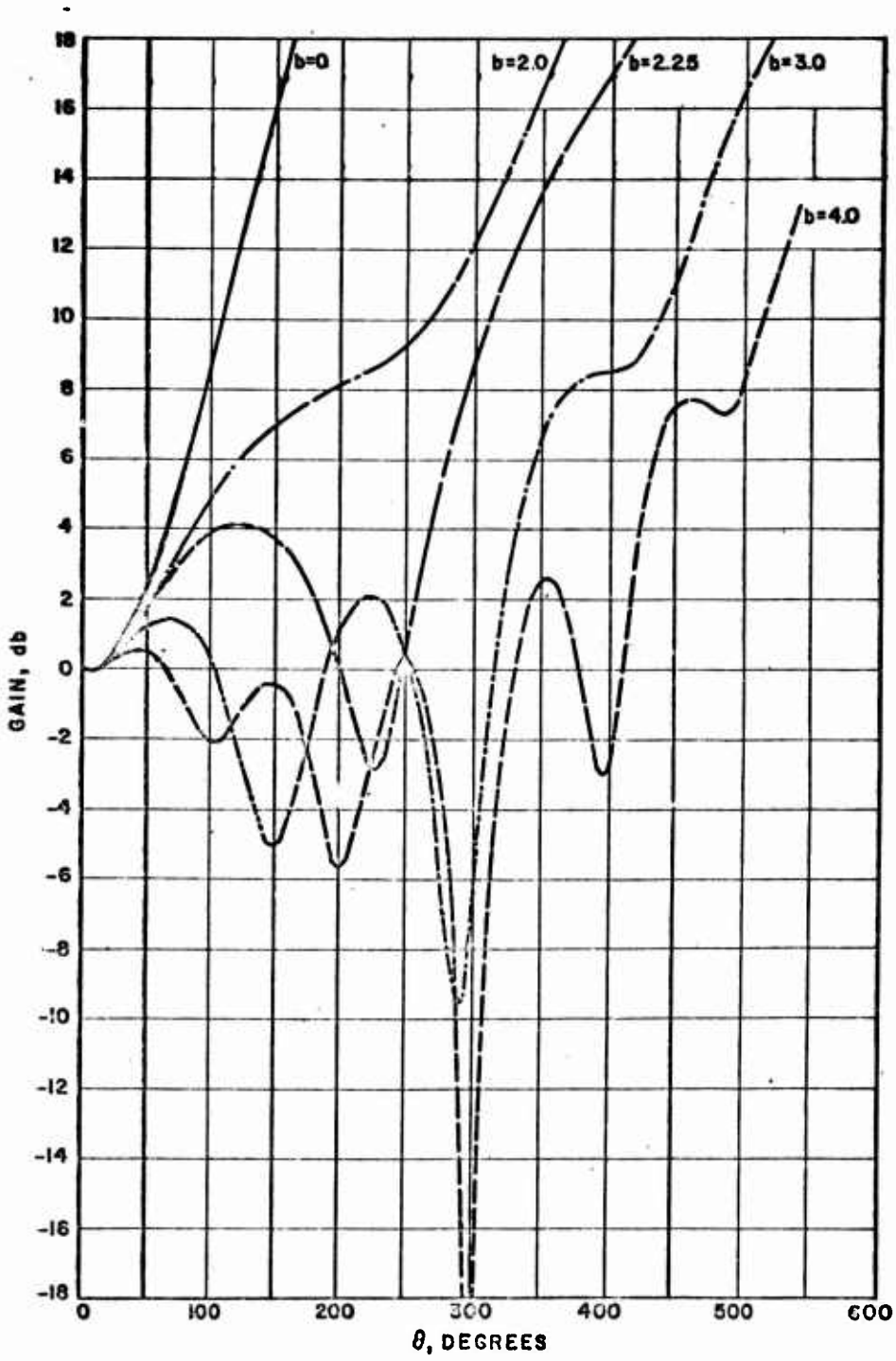

FIG. 5.6 GAIN VS. θ FOR THE M-TYPE AMPLIFIER. (H=1, r=0.5, d=0.1)

The effect of circuit loss on the beating-wave amplification is summarized in Fig. 5.7 where the gain at the first maximum is shown as a function of d for particular values of H and r. If there were no stream present the signal on a lossy circuit would decrease according to

$$\text{Loss in db} = 54.6\,DNd \qquad (5.3)$$

Since the typical M-type beating-wave amplifier length is DN = 0.4 then the signal will decrease at the approximate of 22 db per unit d. It is seen in Fig. 5.7 that with the stream present the gain is reduced at a rate of 24 db per unit d. This is about the same result as obtained in the case of the O-type Crestatron.

6. M-Type BWO Start-Oscillation Conditions (J. E. Rowe)

In the previous progress report a brief outline was given of the method of obtaining the start-oscillation conditions in an M-type BWO when a simple one-level treatment of the input boundary value problem is utilized. In the past period the secular equation and the gain equation were programmed for solution on a digital computer and various start-oscillation conditions were found when there was no circuit loss. The equations used are summarized below. The secular equation has been previously given as

$$(\ell - b)\left[\ell^2 - 2\frac{H-1}{H+1}r\ell + r^2\right] - \ell = 0 \qquad (6.1)$$

where $\ell = \mu - j\nu$. It is convenient to convert the perturbation propagation constant ℓ to the more convenient δ, used by Pierce[1], Muller[2], etc. This is accomplished by substituting $\delta = j\ell$ in Eq. 6.1.

---

1. Pierce, J. R., Traveling-Wave Tubes, D. Van Nostrand Co., New York; 1950.

2. Muller, M., "Traveling-Wave Amplifiers and Backward-Wave Oscillators", Proc. IRE, Vol. 42, pp. 1651-1658; November, 1954.

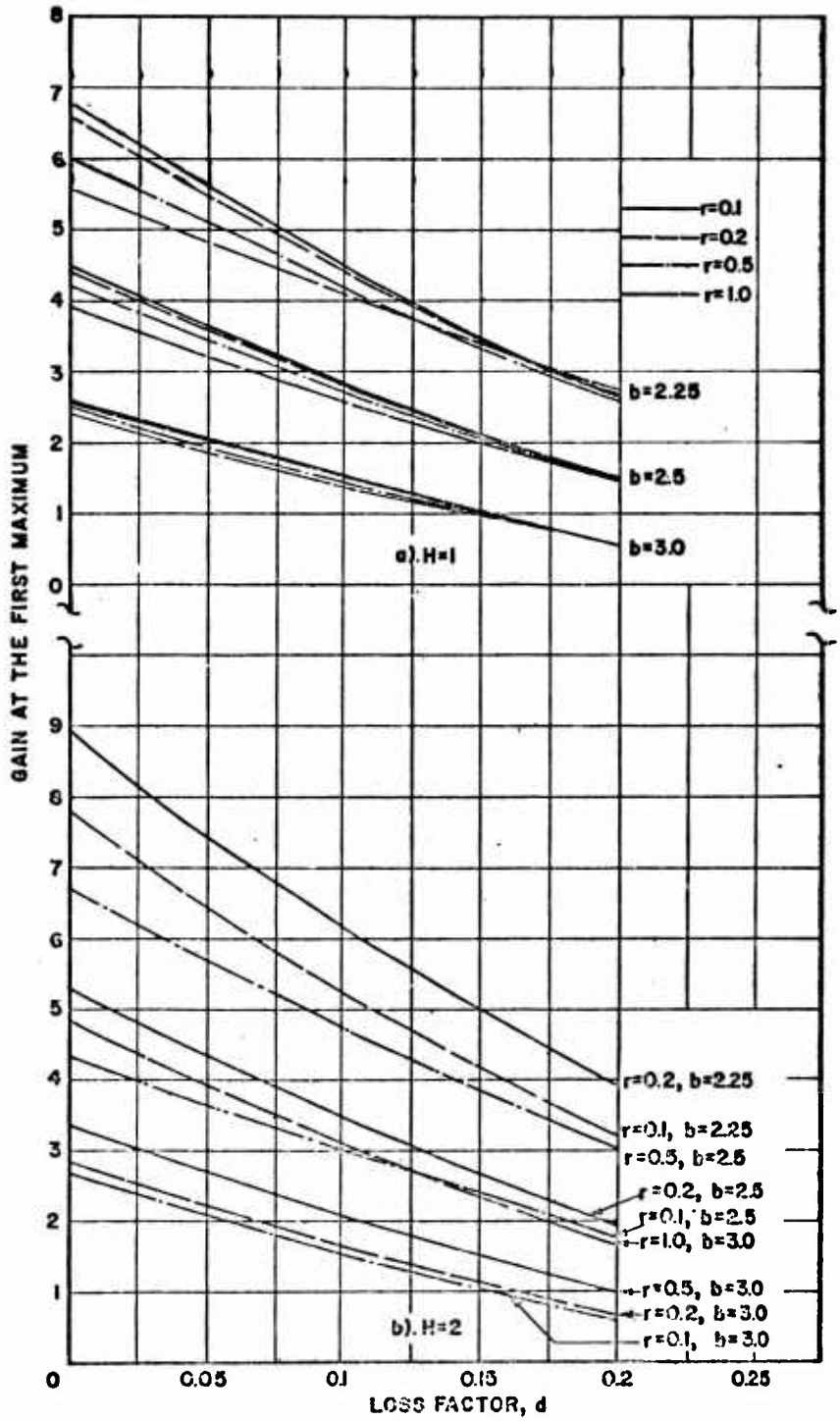

FIG. 5.7 EFFECT OF LOSS ON M-TYPE BEATING-WAVE AMPLIFICATION.

If this change is made and the equation is expanded in polynomial form the following result is obtained. The effect of circuit loss is also included.

$$\delta^3 - j\left[2r\left(\frac{H-1}{H+1}\right) + (b+jd)\right]\delta^2 - \left[r^2 + 2r(b+jd)\left(\frac{H-1}{H+1}\right) - 1\right]\delta$$

$$+ j(b+jd)r^2 = 0 \qquad (6.2)$$

where

$$\delta = x + jy$$

and

d = the circuit loss parameter.

It is important to note that when r = 0 the above equation reduces to the following independent of H.

$$\delta^2 - jb\delta + 1 = 0$$

and

$$\delta = 0 \ . \qquad (6.3)$$

In this case one root is zero, hence there can only be two waves on the circuit.

The matrix to express the input boundary conditions is given below.

$$\begin{bmatrix} 1 & 1 & 1 \\ S_n - 1 & S_{n+1} - 1 & S_{n+2} - 1 \\ \frac{jS_n}{\delta_n} & \frac{jS_{n+1}}{\delta_{n+1}} & \frac{jS_{n+2}}{\delta_{n+2}} \end{bmatrix} \begin{bmatrix} V_n \\ V_{n+1} \\ V_{n+2} \end{bmatrix} = \begin{bmatrix} V_a \\ 0 \\ 0 \end{bmatrix} \qquad (6.4)$$

where

$$\delta_{n+3} \equiv \delta_n$$

and

$$S_n = -(r - j\delta_n)(b + j\delta_n) \ .$$

A solution of the above matrix for the wave amplitudes gives

$$\frac{V_n}{V_a} = \frac{X_n}{\sum_{n=1}^{3} X_n} \tag{6.5}$$

where

$$X_n = \frac{j(S_{n+1}-1)S_{n+2}}{\delta_{n+2}} - \frac{j(S_{n+2}-1)S_{n+1}}{\delta_{n+1}}$$

The r-f voltage as a function of distance can be expressed as

$$\frac{V_t(\theta)}{V_a} = e^{-j\frac{\theta}{D}} \sum_{n=1}^{3} \frac{V_n}{V_a} e^{-\theta\delta_n} \tag{6.6}$$

where $\theta = 2\pi DN$. In order to determine the start-oscillation conditions for particular values of r and H it is necessary to determine values (combinations) of b and θ such that the right hand side of Eq. 6.6 is zero. A convergent process has been developed to determine these points in the b,θ plane. A summary of the first-order starting conditions for the M-type BWO is shown in Figs. 6.1 and 6.2 for various values of the space-charge parameter and the beam position parameter. The space-charge parameter r is identical to Gould's[3] space-charge parameter S. The beam position parameter is defined somewhat differently such that H = 1 corresponds to g = 0. The starting conditions shown are for d = 0. Values for $d \neq 0$ are presently being computed.

It was shown earlier that when r = 0 the secular equation has one zero root and the others are the roots of a quadratic. Under the conditions of H = 1, Dombrowski has shown that the starting condition is

---

3. Gould, R. W., "Space Charge Effects in Beam-Type Magnetrons", J.A.P., Vol. 28, pp. 599-605; May, 1957.

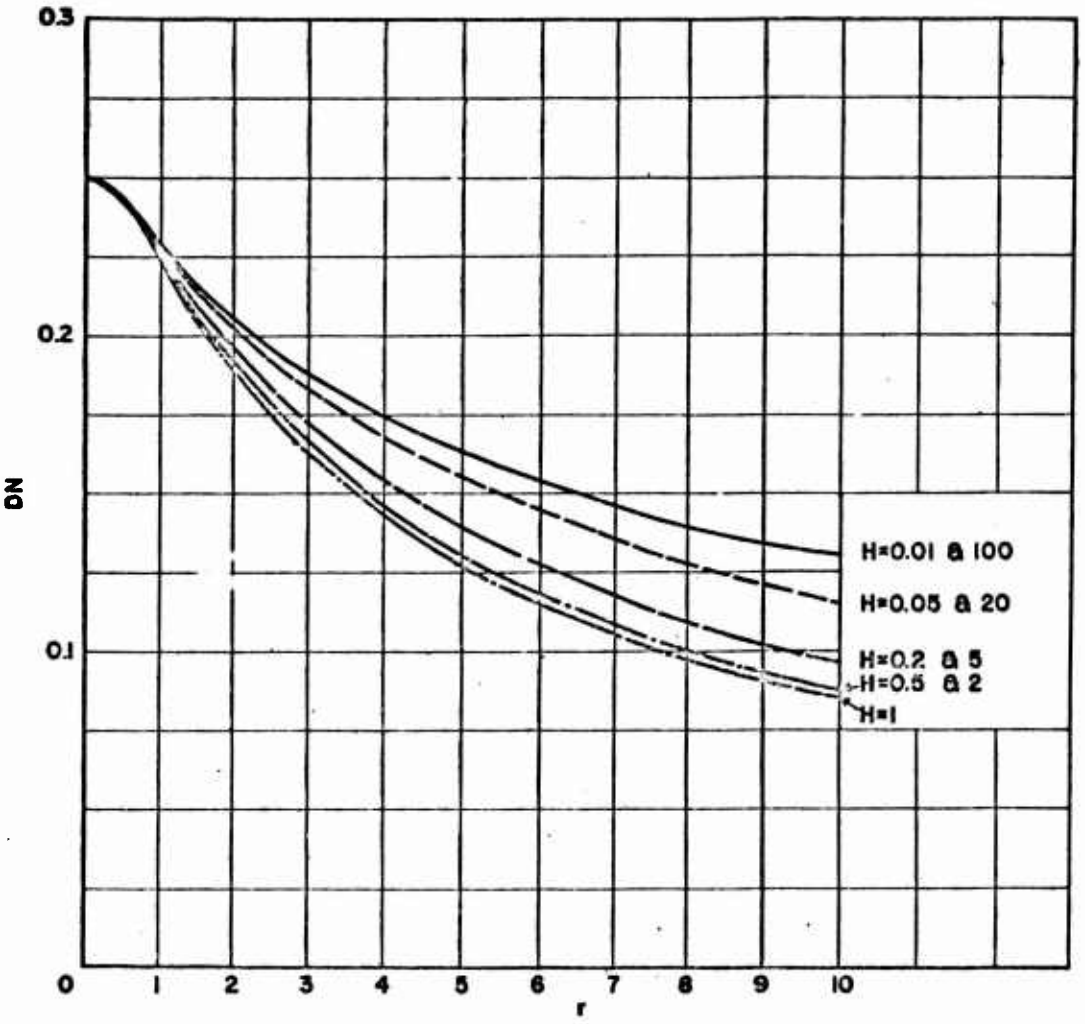

FIG. 6.1 M-TYPE BWO START-OSCILLATION CONDITIONS. (d=0)

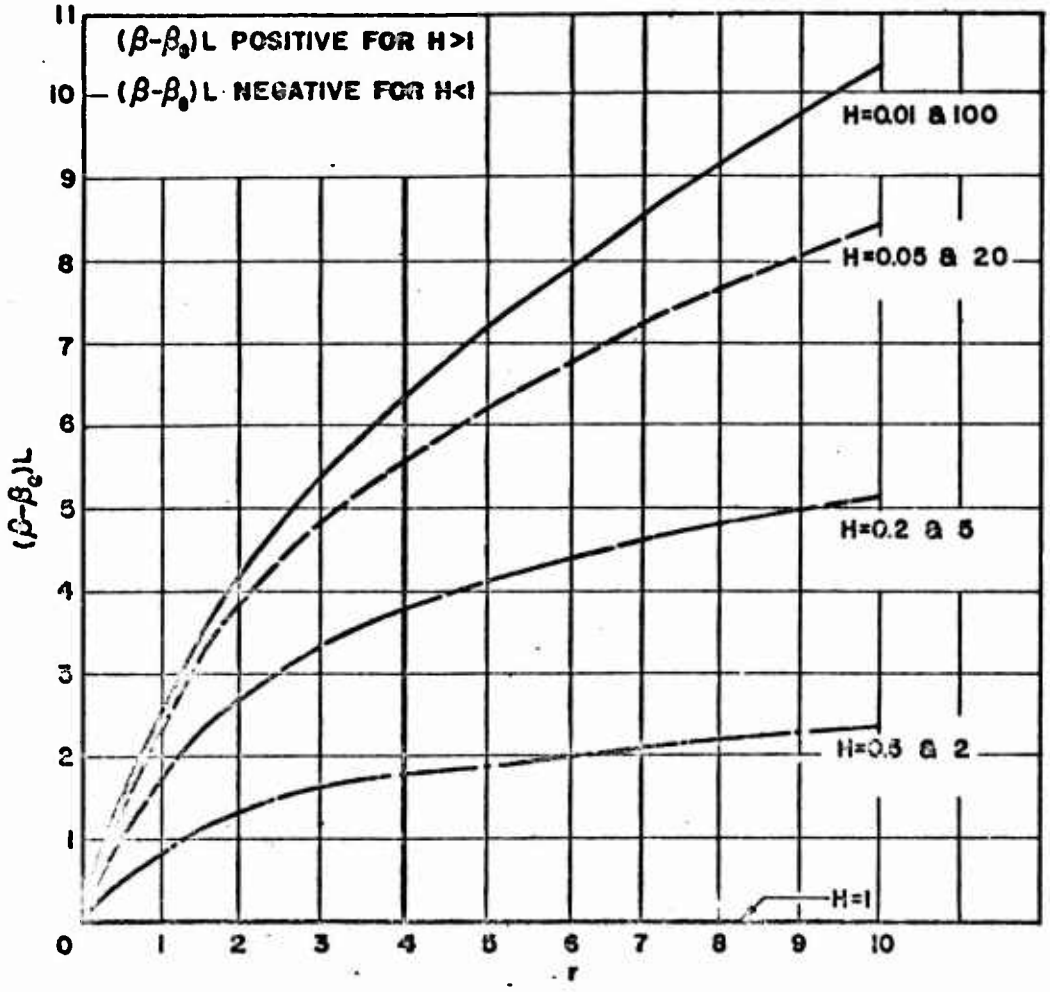

FIG. 6.2 $(\beta-\beta_0)L$ VS. r AT START OSCILLATION. (d=0)

$$DN = \frac{\cos^{-1} r^2}{2\pi\sqrt{1-r^2}} \quad . \qquad (6.7)$$

when r = 0, DN = 0.25, and since the secular equation is independent of H for r = 0 this value applies for all H at r = 0.

When H = 1 the beam is located exactly midway between the circuit and the sole electrodes. It is noticed that the values of DN at starting are the same for beams located symmetrically above and below the centerline between the circuit and sole. On the other hand, the beam must be operated below synchronism with the circuit wave if it is located above the centerline, and above synchronism if it is located below the centerline. This dependence is shown in Fig. 6.2. The results agree with the simple theory of Muller and the more general work of Gould. Additional calculations are being carried out for finite values of circuit loss, a condition not investigated by other authors.

Another objective of determining the start-oscillation conditions for various values of beam position, space charge and circuit loss is to use them as a basis of comparison for starting conditions computed using a variational procedure to account for the effect of the cut-off waves at the input boundary. This alternate treatment of the input boundary value problem minimizes the energy density associated with the cut-off waves. This method of calculating the wave amplitudes excited was used by Hershenov in his field analysis of the magnetron amplifier. He did not apply this technique to the backward-wave oscillator. A circuit analysis using this variational procedure has been developed and currently the program for calculating the start-oscillation conditions is being checked out.

During the next quarter the calculation of start-oscillation conditions for finite values of circuit loss using the simple one-level treatment of the input boundary will be completed. Also it is planned to carry out initial calculations of starting conditions using the variational treatment of the input boundary value problem.

7. Multiple-Stream M-Type Devices (O. P. Gandhi)

In the previous progress report the small-signal dispersion equations for the double-beam M-type amplifier were developed and the solutions for a few cases of such a device were presented. It is recognized that the enhanced growth factor of such devices over those of a single-beam tube is due to the space-charge interaction between the electron bunches of the two individual beams interacting with the crossed electric and magnetic fields. The said space-charge interaction between these bunches results in the repulsive force between them causing the electron bunch of the upper electron beam to move, on the average, closer to the slow-wave structure (this gives a growing wave with a larger growth factor) and the electron bunch of the lower beam to move, on the average, further away from the slow-wave structure (this tendency retards the normal growth that could be obtained from this beam acting alone and gives a growing wave with smaller growth factor). The validity of the above reasoning can be clearly seen from the results presented in Figs. 7.1 through 7.7. In Fig. 7.1 the two growth factors for the double-beam tube for various inter-beam separations are presented. The growth factors for the tube degenerate asymptotically to the values for individual beams for large inter-beam separation.

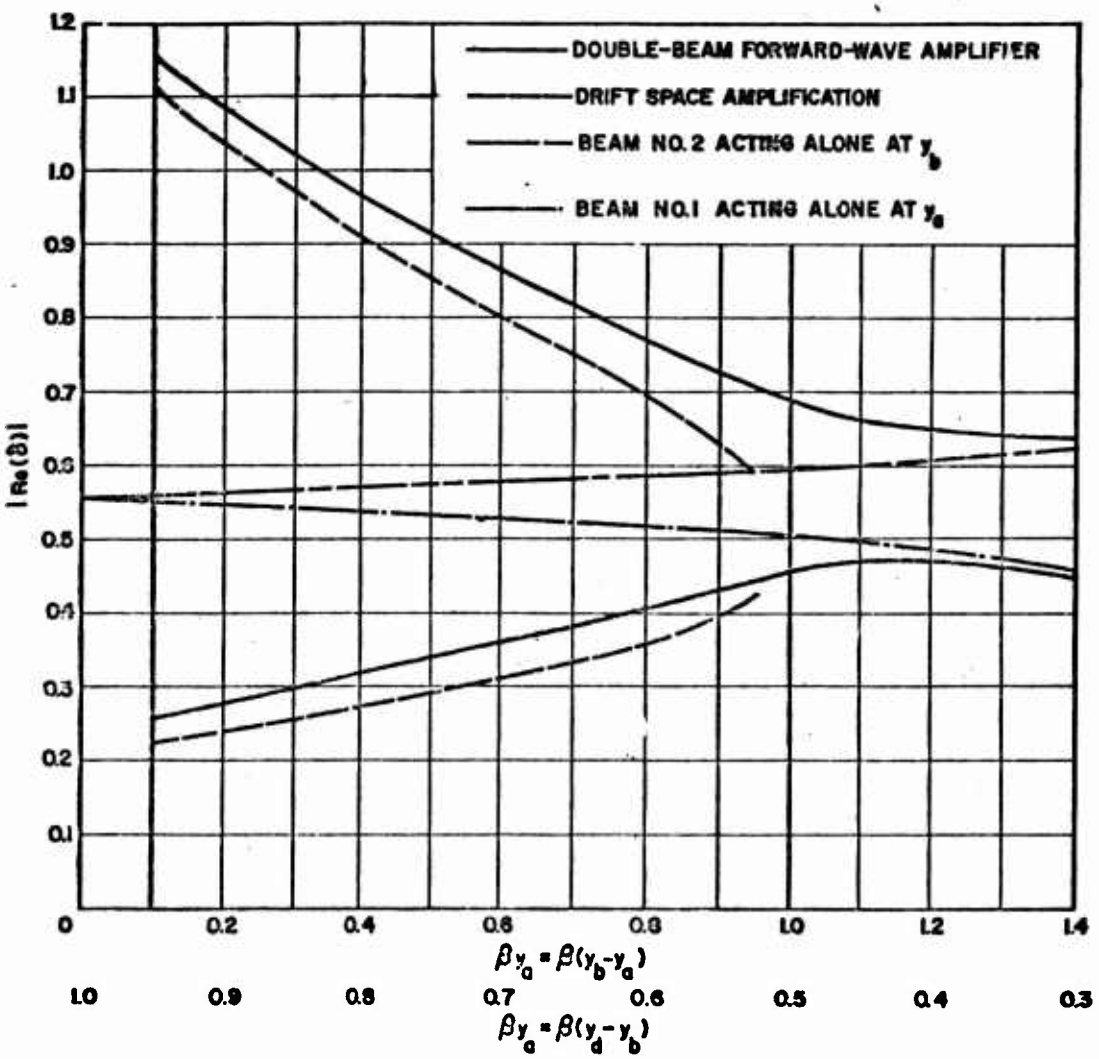

FIG. 7.1 GROWTH FACTORS VS. INTERBEAM SPACING FOR A DOUBLE-BEAM CROSSED-FIELD AMPLIFIER. ($\beta y_d = 2.0$, $\beta \bar{y} = 1.0$, $D = 0.1$, $S_1 = S_2 = 0.5$, $b = 0$)

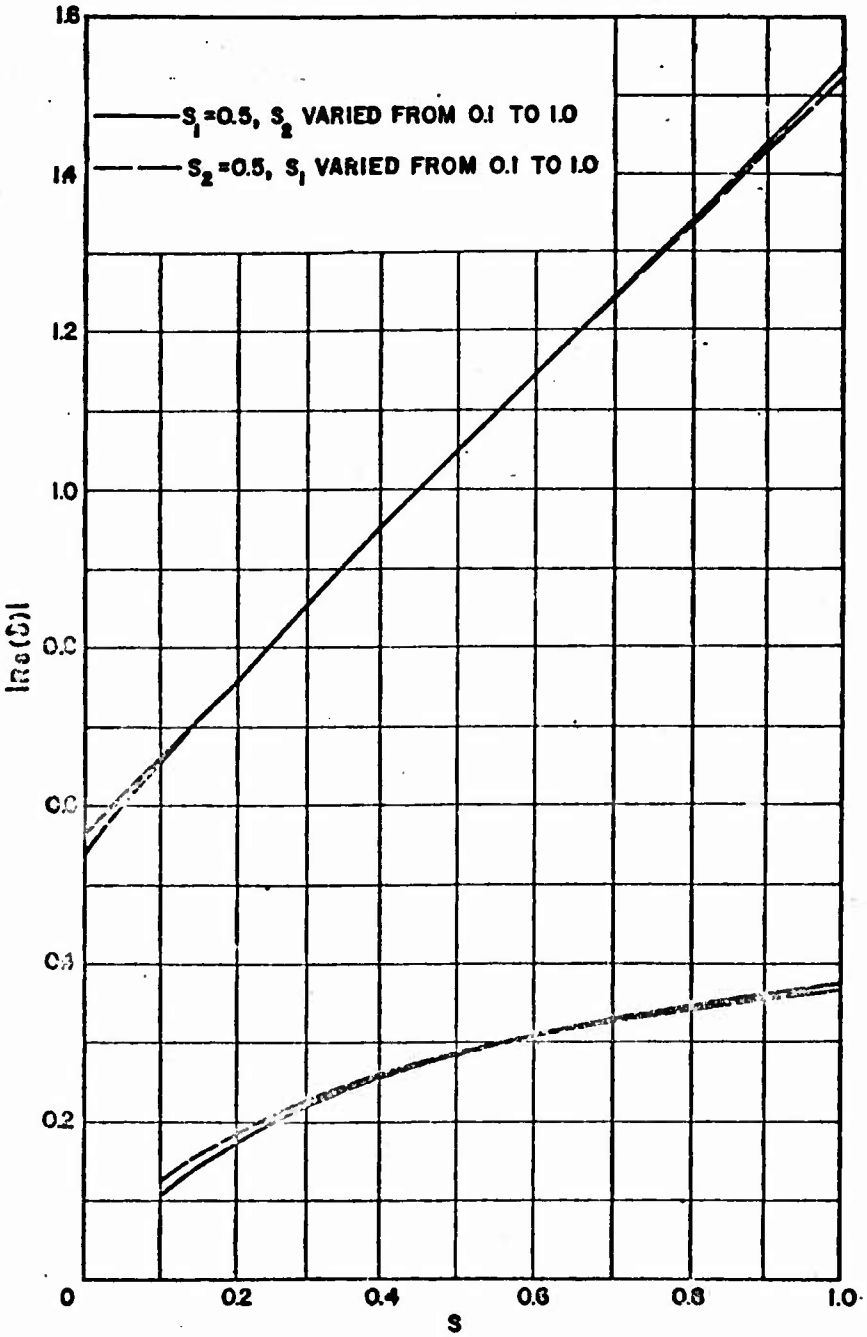

FIG. 7.2 GROWTH FACTORS FOR THE DOUBLE-BEAM CROSSED-FIELD AMPLIFIER. (βy_3=0.875, βy_b=1.125, ζ=4.6, βd=2.0, D=0.1, b=0)

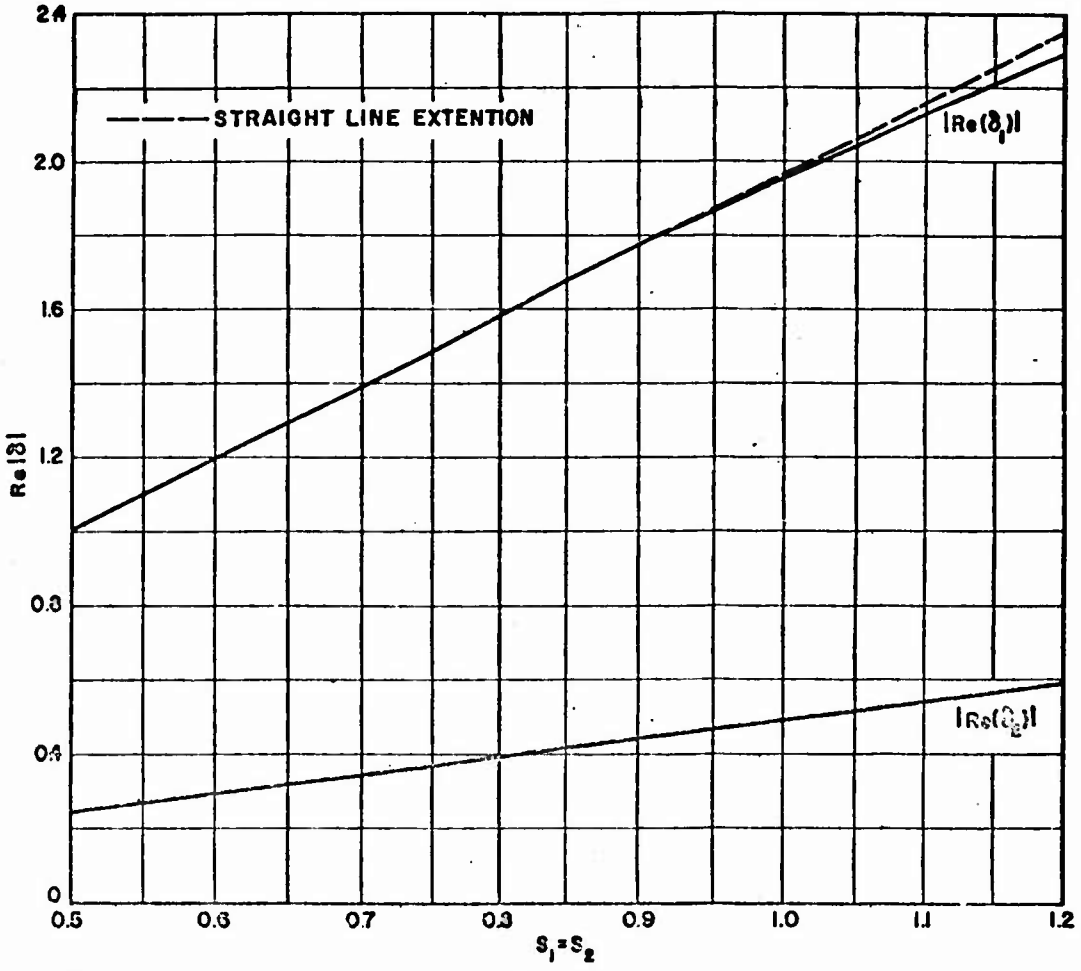

FIG. 7.3 DRIFT REGION GROWTH FACTORS AS A FUNCTION OF SPACE CHARGE. ($\beta_0 v_0$=0.875, $\beta_0 v_b$=1.125, D=0.1, b=0, $S_1=S_2$)

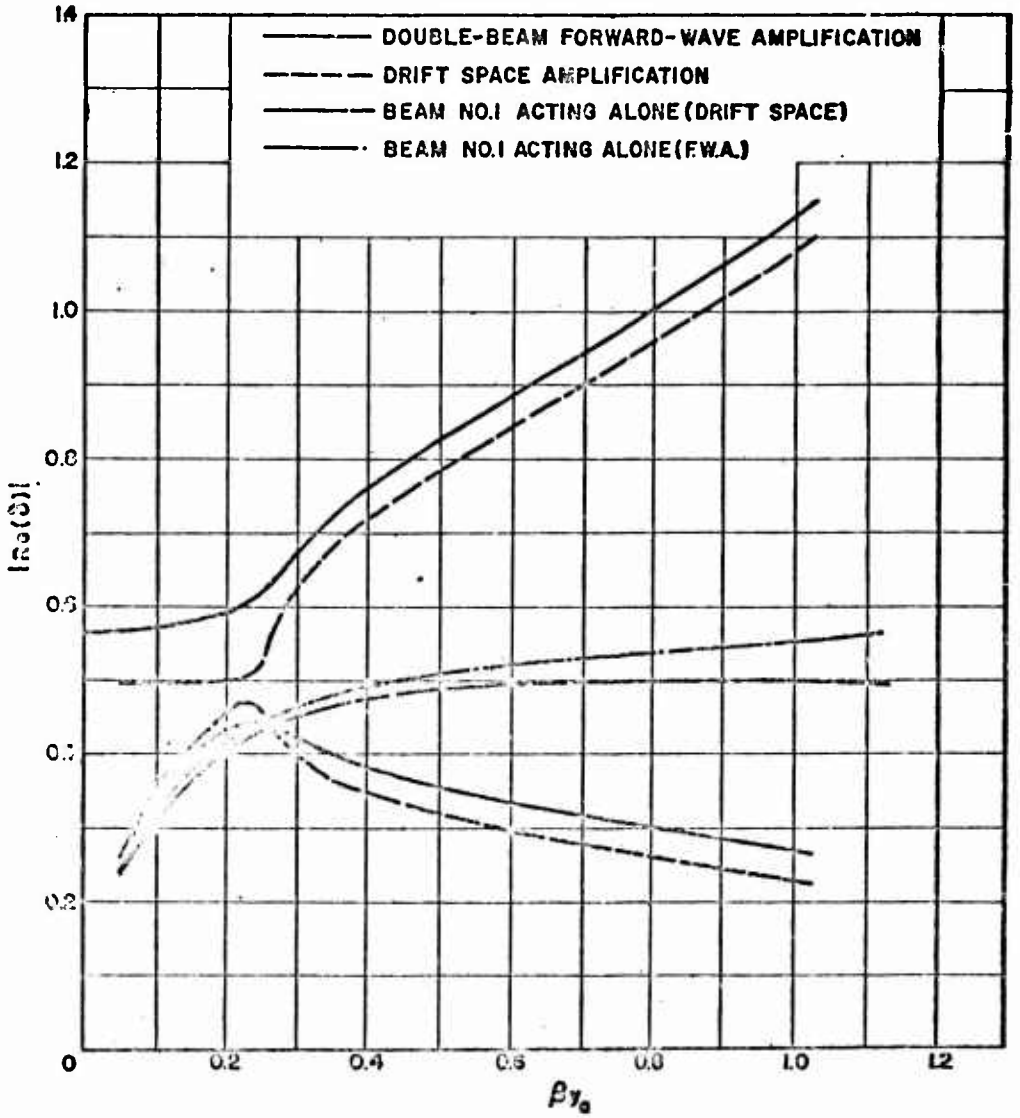

FIG. 7.4 DOUBLE-BEAM CROSSED-FIELD AMPLIFIER GROWTH FACTORS. ($\beta y_d = 2.0$, $\beta y_b = 1.125$, $D = 0.1$, $S_1 = S_2 = 0.5$, $b = 0$)

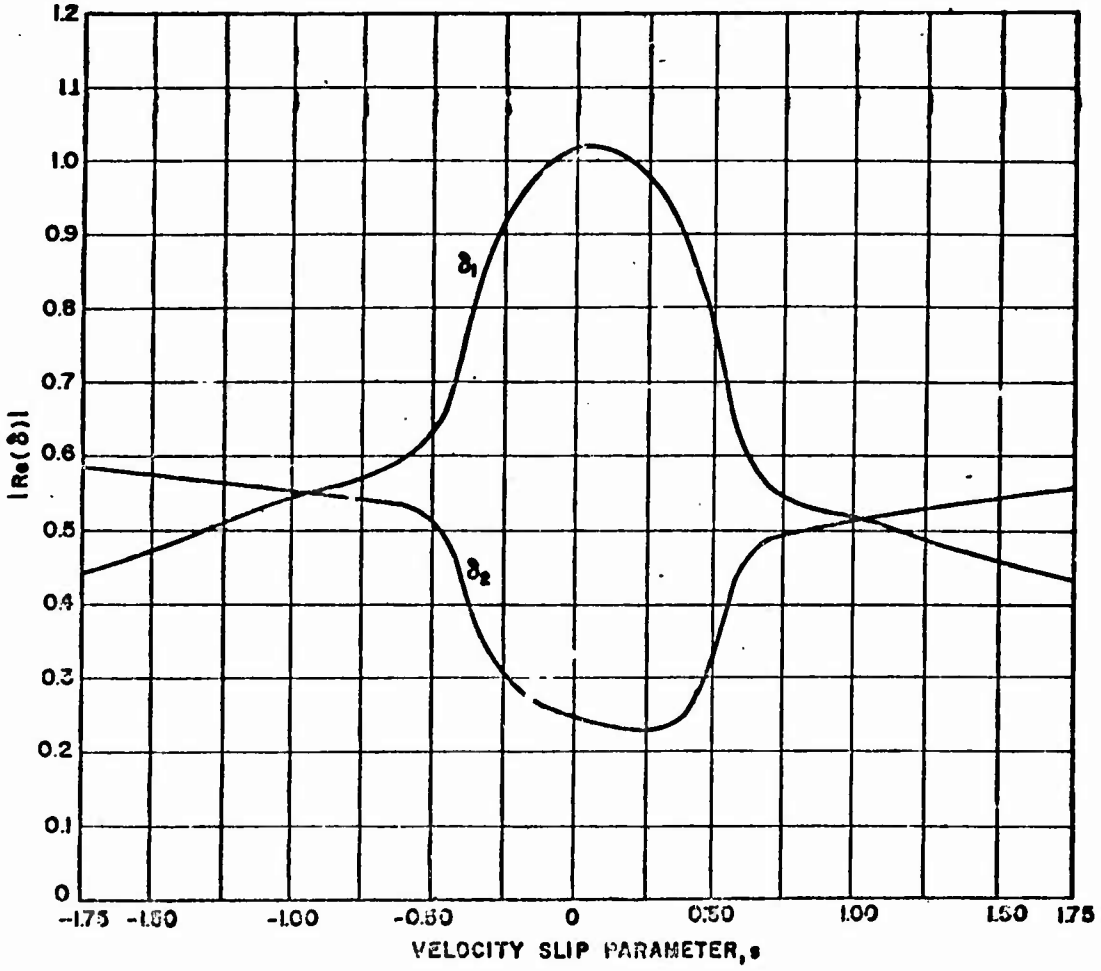

FIG. 7.5 GROWTH FACTORS VS. VELOCITY SLIP PARAMETER s OF THE DOUBLE-BEAM FORWARD-WAVE AMPLIFIER. ($S_1 = S_2 = 0.5$, $\beta_0 y_a = 0.875$, $\beta_0 y_b = 1.125$, $\beta_0 d = 2.0$, $\zeta = -4.8$, $b = -1.0$)

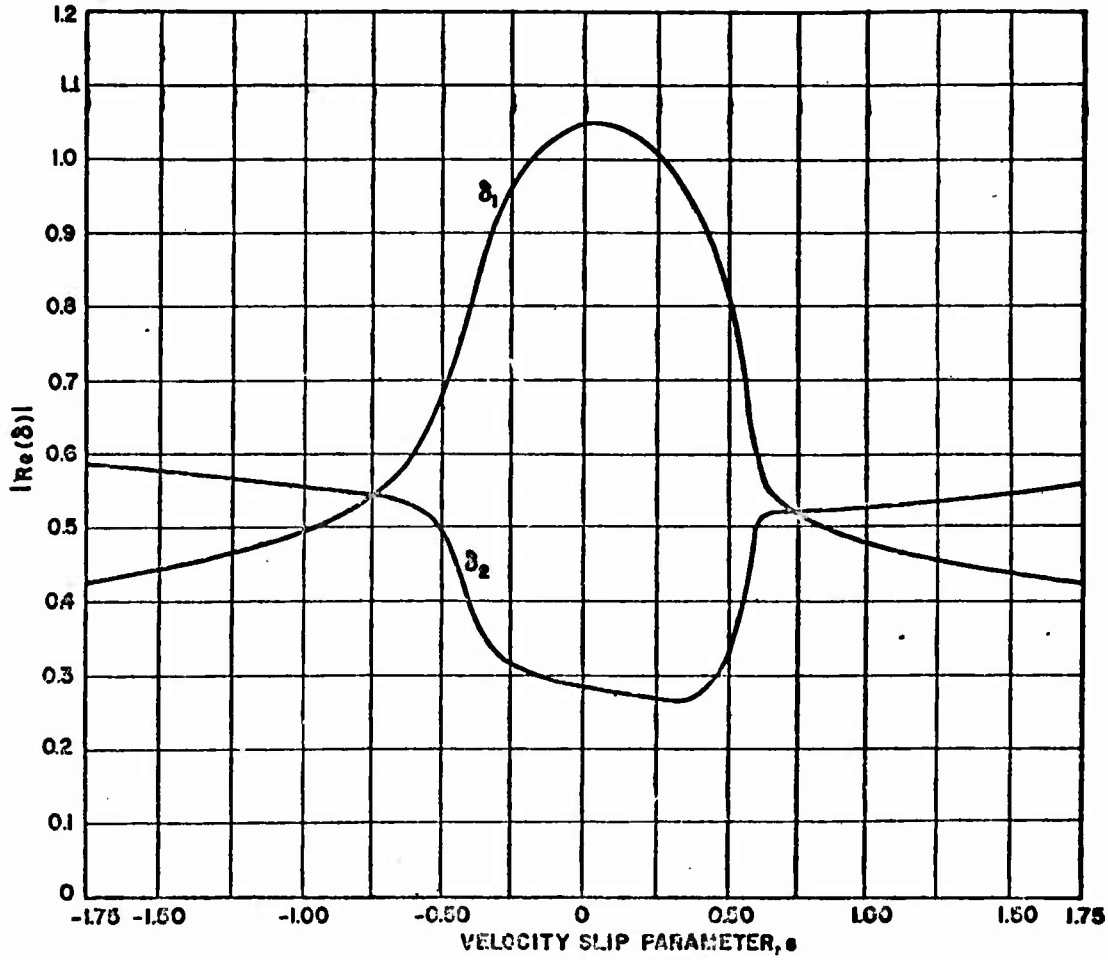

FIG 7.6 GROWTH FACTORS VS. VELOCITY SLIP PARAMETER s OF THE DOUBLE-BEAM FORWARD-WAVE AMPLIFIER. ($S_1=S_2=0.5$, $\beta_0 y_a=0.875$, $\beta_0 y_b=1.125$, $\beta_0 d=2.0$, $\zeta=4.8$, $b=0$)

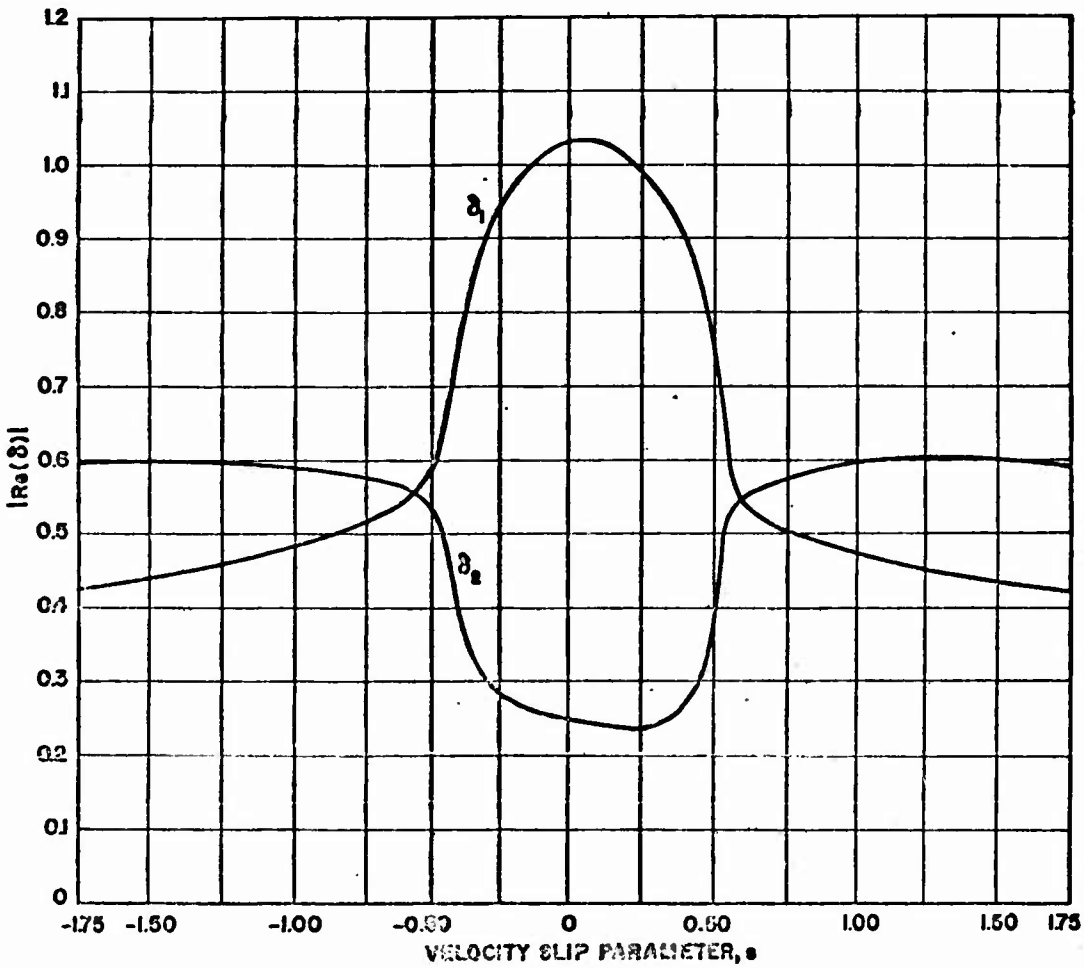

FIG. 7.7 GROWTH FACTORS VS. VELOCITY SLIP PARAMETER s OF THE DOUBLE-BEAM FORWARD-WAVE AMPLIFIER. ($S_1=S_2=0.5$, $\beta_0 y_a=0.875$, $S_2=1.25$, $\beta_0 d=2.0$, $\zeta=4.8$, $b=1.0$)

Since the space-charge interaction between electron bunches of the two beams is proportional to the d-c space-charge densities of the individual beams (space-charge parameters S_1 and S_2), it is expected that the difference between the two growth factors of the double-beam tube should vary as a linear function of the space-charge parameter. That this is so can be seen from the results for the double-beam forward-wave amplifier and drift-tube amplifier presented in Figs. 7.2 and 7.3 respectively.

Presented in Fig. 7.4 are the variations of the growth factors for various entrance positions of beam No. 1 (beam No. 2 entering the interaction region at a fixed plane) both for the forward-wave and drift-tube amplifiers.

Since the double-beam crossed-field amplifer depends upon the space-charge interaction between electron bunches of the two beams, the multiple-beam interaction and hence the growth factor of the faster growing wave should reduce if the entrance velocities of the two beams are unequal.

If the relative slip parameter, s, of the two beams is defined as:

$$s = \frac{\bar{u} - u_2}{u_2 D}$$

where

$$\bar{u} = \frac{2 u_1 u_2}{u_1 + u_2} ,$$

then the dispersion equations for the double-beam crossed-field amplifier are as follows.

Double-beam forward-wave amplifier with slow-wave structure:

$$\left[\frac{s - S_2 - j\delta(1+S_2D)}{s + S_2 - j\delta(1-S_2D)}\right]^2 \cdot$$

$$\cdot \frac{\coth \beta_o y_d - \tanh \beta_o(y_d-y_b) - \frac{j\zeta}{1+Db}(\delta+jb)}{1 - \tanh \beta_o(y_d-y_b) \coth \beta_o y_d + \frac{j\zeta}{1+Db}(\delta+jb) \tanh \beta_o(y_d-y_b)}$$

$$= \frac{[s - S_1 + j\delta(1-S_1D)]^2 + [s + S_1 + j\delta(1+S_1D)]^2 \tanh \beta_o y_a \tanh \beta_o(y_b-y_a)}{[s - S_1 + j\delta(1-S_1D)]^2 \tanh \beta_o(y_b-y_a) + [s + S_1 + j\delta(1+S_1D)]^2 \tanh \beta_o y_a} \cdot \tag{7.1}$$

Double-beam amplifier drift-space amplification:

$$\cdot \left[\frac{s - S_2 - j\delta(1+S_2D)}{s + S_2 - j\delta(1-S_2D)}\right]^2 \coth \beta_o(y_d-y_b)$$

$$= \frac{[s - S_1 + j\delta(1-S_1D)]^2 + [s + S_1 + j\delta(1+S_1D)]^2 \tanh \beta_o y_a \tanh \beta_o(y_b-y_a)}{[s - S_1 + j\delta(1-S_1D)]^2 \tanh \beta_o(y_b-y_a) + [s + S_1 + j\delta(1+S_1D)]^2 \tanh \beta_o y_a} \tag{7.2}$$

where

$$\beta = \bar{\beta}(1+jD\delta)$$

$$\bar{\beta} = \frac{\beta_1 + \beta_2}{2} \; ; \; \beta_1 = \frac{\omega}{u_1} \; ; \; \beta_2 = \frac{\omega}{u_2}$$

and

$$\bar{u} = v_o(1+Db) \; .$$

All other quantities are defined in a manner similar to those in the previous progress report. Equations 7.1 and 7.2 degenerate respectively to Eqs. 7.16 and 7.17 of the previous progress report for the case $s = 0$ (i.e., when the entrance velocities of the two beams are equal).

The growth factors of the double-beam forward-wave amplifier for various values of the slip parameter s are presented for the three cases

b = -1.0, 0, 1.0 in Figs. 7.5 through 7.7. It can be seen that the growth factor of the faster growing wave decreases for increasing values of the slip parameter as would be expected from the above reasoning.

In order to find the gain of the double-beam amplifier we need to find the amplitudes of the excited waves from the input boundary conditions. These are obtained by matching a-c beam displacement $\tilde{y}$ and the a-c charge density at the center of the two beams to those of the beams entering the tube. The choice of $\tilde{y}$ and $\tilde{\sigma}$ for matching conditions as against the a-c components of y- and z-directed velocities is dictated by the fact that the latter quantities are very weakly excited especially for synchronous waves ($\delta \to 0$) and the error in the determination of the amplitudes A_i could be considerable. The fifth equation in the case of a tube with a slow-wave structure to the amplitude of the incoming signal. The five determinantal equations for the amplitudes A_i take the form:

$$\sum_{i=1}^{5} \frac{s + j\delta_i}{\delta_i(d_i + j\delta_i e_i)} A_i \sinh \beta_i y_a = \frac{\omega_c}{\eta} \omega D \tilde{y}_1 \tag{7.3}$$

$$\sum_{i=1}^{5} \frac{(s+j\delta_i)(1+jD\delta_i)}{\delta_i(a_i + j\delta_i b_i)} A_i \cosh \beta_i y_a = -\frac{1}{2\epsilon_o S_1} \tilde{\sigma}_1 \tag{7.4}$$

$$\sum_{i=1}^{5} \frac{s - j\delta_i}{\delta_i(a_2 - j\delta_i e_2)} A_i \left[\frac{d_i + j\delta_i e_i}{a_i + j\delta_i b_i} \cosh \beta_i y_a \sinh \beta_i (y_b - y_a) + \frac{a_i + j\delta_i b_i}{d_i + j\delta_i e_i} \sinh \beta_i y_a \cosh \beta_i (y_b - y_a) \right] = \frac{\omega_c}{\eta} \omega D \tilde{y}_2 \tag{7.5}$$

$$\sum_{i=1}^{5} \frac{(s-j\delta_i)(1+jD\delta_i)}{\delta_i(d_1-j\delta_i e_1)} A_i\left[\frac{d_1 + j\delta_i e_1}{a_1 + j\delta_i b_1} \cosh \beta_i y_a \cosh \beta_i(y_b-y_a)\right.$$

$$\left. + \frac{a_1 + j\delta_i b_1}{d_1 + j\delta_i e_1} \sinh \beta_i y_a \sinh \beta_i(y_b-y_a)\right] = -\frac{1}{2\epsilon_o S_2} \tilde{\sigma}_2 \qquad (7.6)$$

and

$$\sum_{i=1}^{5} \tilde{V}_i = V_o \qquad (7.7)$$

where

$$a_1 = s + S_1; \qquad a_2 = s + S_2$$

$$b_1 = 1 + S_1 D; \qquad b_2 = 1 + S_2 D$$

$$d_1 = s - S_1; \qquad d_2 = s - S_2$$

$$e_1 = 1 - S_1 D; \qquad e_2 = 1 - S_2 D \ .$$

and

V_o is the amplitude of the incoming r-f signal.

Solution of Eqs. 7.3 through 7.7 for the ith wave amplitude yields

$$V_i = -\frac{j A_i}{\beta_i}\left[\frac{d_2 - j\delta_i b_2}{a_2 - j\delta_i e_2} B_i \cosh \beta_i(y_d-y_b)\right.$$

$$\left. + \frac{a_2 - j\delta_i e_2}{d_2 - j\delta_i b_2} C_i \sinh \beta_i(y_d-y_b)\right] \qquad (7.8)$$

where B_i and C_i are given by

$$B_i = \frac{d_1 + j\delta_i b_1}{a_1 + j\delta_i b_1} \cosh \beta_i y_a \sinh \beta_i(y_b-y_a)$$

$$+ \frac{a_1 + j\delta_i b_1}{d_1 + j\delta_i e_1} \sinh \beta_i y_a \cosh \beta_i(y_b-y_a) \ .$$

and

$$C_i = \frac{d_i + j\delta_i e_i}{a_i + j\delta_i b_i} \cosh \beta_i y_a \cosh \beta_i (y_b - y_a)$$

$$+ \frac{a_i + j\delta_i b_i}{d_i + j\delta_i e_i} \sinh \beta_i y_a \sinh \beta_i (y_b - y_a) \quad .$$

The quantities $\tilde{y}_1$, $\tilde{\sigma}_1$, $\tilde{y}_2$ and $\tilde{\sigma}_2$ denote the a-c beam displacement and a-c charge density of the beams at entrance and are zero for the unmodulated entering streams. Equations 7.3 through 7.7 above are solved simultaneously for the r-f wave amplitudes A_i. For the double-stream drift-space amplifier case only four waves are excited and their amplitudes are determined from the simultaneous solution of Eqs. 7.3 through 7.6.

During the next quarter it is planned to obtain the amplitudes of the excited waves in the double-stream tube. Large-signal behavior of the double-stream forward-wave amplifier will also be studied. The large equations to be used for this are the general large-signal crossed-field device equations derived by Gandhi and Rowe[1].

8. Conclusions (J. E. Rowe)

A crossed-field stream analyzer with a modified cathode structure was completed and initial tests verified the general nature of Miller's earlier results. Some experiments have been carried out in which electrons were drawn into the potential trap in the sole electrode. Analog computer solutions for electron trajectories moving into the potential trap were found.

---

1. Gandhi, O., Rowe, J. E., "Large-Signal Analysis of Crossed-Field Devices", Semiannual Progress Report No. 1, Electron Physics Laboratory, Department of Electrical Engineering, The University of Michigan; August 1959.

Extensive studies and computations of beating-wave amplification in M-type amplifiers were carried out and this type of amplification was shown to exist for finite values of the space charge and loss parameters. The effect of circuit loss on the beating-wave gain was shown to be the same as for the O-type Crestatron.

Calculation of M-type BWO starting conditions was carried out and it was found that the DN for start oscillation was the same for H and 1/H at all values of r. If the stream is located above the midplane between the sole and the circuit then b is negative at start oscillation and if the beam is below the midplane then b is positive at start oscillation when H = 1, b = 0 at start oscillation independent of r.

The dispersion equation for the double-beam crossed-field amplifier was modified to account for a slip between the two beams. Solutions of the dispersion equation indicate that there is a space-charge interaction between the two streams in which the coulomb force between bunches in the two streams causes the upper bunch to move closer to the circuit and enhances the growth mechanism.

DISTRIBUTION LIST

No. Copies	Agency
3	Project Engineer, Electronic Components Research Department, U. S. Army Signal Research & Development Laboratory, Fort Monmouth, New Jersey, ATTN: SIGFM/EL-PR
1	Mail & Records, Electronic Components Research Department, U. S. Army Signal Research & Development Laboratory, Fort Monmouth, New Jersey
1	Commanding General, U. S. Army Signal Research & Development Laboratory, Fort Monmouth, New Jersey, ATTN: Director of Research/or Engineering
1	Commanding General, U. S. Army Signal Research & Development Laboratory, Fort Monmouth, New Jersey, ATTN: Chief, Technical Documents Center
1	Commanding General, U. S. Army Signal Research & Development Laboratory, Fort Monmouth, New Jersey, ATTN: Adjutant Branch; Mail, File & Records
3	Commanding General, U. S. Army Signal Research & Development Laboratory, Fort Monmouth, New Jersey, ATTN: Chief, Technical Information Division (FOR RETRANSMITTAL TO ACCREDITED BRITISH AND CANADIAN GOVERNMENT REPRESENTATIVES)
3	Continental Army Command Liaison Office, U. S. Army Signal Research & Development Laboratory, Fort Monmouth, New Jersey
1	Commanding Officer, U. S. Army Signal Equipment Support Agency, Fort Monmouth, New Jersey, ATTN: SIGFM/ES-ASA
1	Chief Signal Officer, Department of the Army, Washington 25, D. C., ATTN: SIGRD
1	Commanding Officer, 9560th TSU, Signal Corps Electronics Research Unit, P. O. Box 205, Mountain View, California
1	Commanding General, U. S. Army Electronic Proving Ground, Fort Huachuca, Arizona
1	Director, U. S. Naval Research Laboratory, Code 2027, Washington 25, D. C.
1	Commanding Officer and Director, U. S. Navy Electronics Laboratory, San Diego 52, California

DISTRIBUTION LIST (Cont.)

No. Copies	Agency
2	Commander, Wright Air Development Center, Wright-Patterson Air Force Base, Ohio, ATTN: WCOSI-3
1	Commander, Air Force Cambridge Research Center, CROTIR-2, L. G. Hanscom Field, Bedford, Massachusetts
1	Commander, Rome Air Development Center, Griffiss Air Force Base, Rome, New York, ATTN: RCSSLD-3
5	Commander, Armed Services Technical Information Agency, Arlington Hall Station, Arlington 12, Virginia
1	Electronics Research Laboratory, Stanford University, Stanford, California, ATTN: Mr. David C. Bacon, Assistant Director
1	Commanding General, Aberdeen Proving Ground, Aberdeen, Maryland, ATTN: Dev. & Proof Svc, Fire Control Div., Capt. Alter
1	Commanding Officer, U. S. Army Signal Research & Development Laboratory, Fort Monmouth, New Jersey, ATTN: Radar Division, Surveillance Dept.
1	Raytheon Manufacturing Company, Foundry Avenue, Waltham 54, Massachusetts, ATTN: W. T. Welsh (SC-71173)
1	Varian Associates, 611 Hansen Way, Palo Alto, California, ATTN: Mrs. Helen Dean, Technical Library
1	Sylvania Electric Products Inc., Mountain View, California, ATTN: Mr. M. Pease
1	University of California, Berkeley 4, California, ATTN: Prof. J. R. Whinnery
1	Bell Telephone Laboratories, Inc., Murray Hill Laboratory, Murray Hill, New Jersey, ATTN: H. M. Olson
1	Signal Corps Liaison Office, Massachusetts Institute of Technology, 77 Massachusetts Avenue, Bldg. 20C-116, Cambridge, Massachusetts, ATTN: A. D. Bedrosian
1	Commanding Officer, Air Force Office of Scientific Research, Washington 25, D. C., ATTN: SRYA
1	Commander, Air Force Cambridge Research Center, Air Research & Development Command, 224 Albany Street, Cambridge 39, Massachusetts, ATTN: Tube Group

DISTRIBUTION LIST (Cont.)

No. Copies	Agency
1	Polytechnic Institute of Brooklyn, Microwave Research Institute, 55 Johnson Street, Brooklyn 1, New York
1	Harvard University, Technical Reports Collection, Room 303A, Pierce Hall, Cambridge 38, Massachusetts, ATTN: M. L. Cox, Librarian
1	University of Illinois, Electrical Engineering Research Laboratory, Urbana, Illinois, ATTN: Technical Editor (Sally Sapper)
1	Ohio State University, Department of Electrical Engineering, Columbus 10, Ohio, ATTN: Professor E. M. Boone
1	General Electric Company, Electron Tube Division of the Research Laboratory, The Knolls, Schenectady, New York, ATTN: E. D. McArthur
1	Hughes Aircraft Company, Electron Tube Laboratory, Culver City, California, ATTN: John Mendel
1	Litton Industries, 1025 Brittan Avenue, San Carlos, California
1	Radio Corporation of America, RCA Laboratories, Princeton, New Jersey, ATTN: Nerguard
1	Sylvania Electric Products, Inc., Physics Laboratory, 208-20 Willetts Point Blvd., Bayside, L. I., New York, ATTN: Louis R. Bloom
1	Commanding Officer, U. S. Army Signal Research & Development Laboratory, Fort Monmouth, New Jersey, ATTN: Technical Information Division, For Retransmittal to: French Military Attache
1	The European Office, U. S. Army R & D Liaison Group, APO 757, New York, New York, For Retransmittal to: Contractor, DA 91-508-EUC-986
1	Dr. Robert T. Young, Chief, Electron Tube Branch, Diamond Ordnance Fuze Laboratories, Washington 25, D. C.
1	Microwave Laboratory, W. W. Hansen Laboratories of Physics, Stanford University, Stanford, California, ATTN: Librarian
1	Sperry Corporation, Electronic Tube Division, Gainesville, Florida, ATTN: Mr. P. Bergman

DISTRIBUTION LIST (Cont.)

No. Copies	Agency
1	Raytheon Manufacturing Company, Microwave and Power Tube Division, Waltham 54, Massachusetts, ATTN: W. C. Brown
1	Polytechnic Institute of Brooklyn, Library, Microwave Research Institute, Brooklyn 1, New York
1	Mr. Gerald Klein, Manager, Microwave Tubes Section, Applied Research Department, Friendship International Airport, Box 746, Baltimore 3, Maryland
1	Mr. W. J. Reigger, Code 691 A4, Microwave Tube Branch, Bureau of Ships, Department of the Navy, Washington 25, D. C.
1	Mr. J. J. Sullivan, Code 691 A4, Microwave Tube Branch, Bureau of Ships, Department of the Navy, Washington 25, D. C.
1	Power Tube Department, 1 River Road, General Electric Company, Schenectady, New York, Attn: Dr. Bernard Hershenov
1	Microwave Electronic Corporation, 4061 Transport Street, Palo Alto, California, Attn: Dr. S. F. Kaisel
1	Librarian, Microwave Library, Stanford University, Stanford, California
1	Westinghouse Electric Corp., P. O. Box 284, Elmira, New York, ATTN: Mr. E. Okress